NTNU – Trondheim
Norwegian University of
Science and Technology

Analysis of Hook load Signal to reveal the Causes of Restrictions

Tina Svensli Glomstad

Earth Sciences and Petroleum Engineering
Submission date: June 2012
Supervisor: Pål Skalle, IPT

Norwegian University of Science and Technology
Department of Petroleum Engineering and Applied Geophysics

Analysis of Hook load Signal to reveal the Causes of Restrictions

Tina Svensli Glomstad
The Department of Petroleum Engineering and Applied Geophysics
NTNU

June 4, 2012

NTNU – Trondheim
Norwegian University of
Science and Technology

Preface

This thesis is written in accordance with the course TPG 4910 Petroleum Engineering - Drilling Technology at the Norwegian University of Science and Technology, Department of Petroleum Engineering and Applied Geophysics.

I would like to thank my supervisor, Professor Pål Skalle, who has given me guidance and support throughout my work on the thesis. I would also like to thank Uduak Mme, Post doc. at NTNU for his help with the laboratory, and Tommy Toverud, NTNU, for guidance regarding simulations in Matlab.

Trondheim, June 4, 2012

Tina Svensli Glomstad

Abstract

Wells that are drilled today are becoming deeper and more complex, and actions to make these wells economically justifiable are desired by oil companies. One method is to reduce the non-productive time during drilling by analysing the hook load response to restrictions in the well. The goal is to recognize abnormal behavior as early as possible to prevent stuck pipe or other incidents that may lead to non-productive time.

In present thesis a mathematical model for simulating hook load during normal tripping conditions is made. The model is based on theory about forces acting in the borehole, and properties of the drill string and the wellbore are inserted into it. The goal is to make good hook load simulations for simple tripping conditions, as restrictions most often cause problems during tripping operations. If restrictions were to occur, the changes in hook load during tripping would be identified quickly, and remedies can be started early.

A laboratory that simulates tripping out of a nearly horizontal well is buildt and experiments are done. The laboratory experiments are carried out with and without mud flow, to identify also the forces that depends on mud circulation. Washout has been imitated in order to see how restrictions affect the hook load. The model consists of mathematical equations that describe all forces acting on the drill string. The laboratory results were used to adjust the equations, so they match hook load behavior even better.

From comparison with the laboratory results it was found that the model creates accurate hook load simulations under simple conditions. Simulations with mud flow during tripping were inaccurate because the forces that occur during circulation were poorly mathematically described in the model. It is not possible to run real time drilling data in the model to see if the model is realistic because block position measurements are missing and some measurement rates are too low, so the equations in the model is not general enough. With improved position measurements and following adjustments in the model, it is likely that the hook load behavior model could be used to reduce the non-productive time during drilling.

Sammendrag

Brønner som blir boret i dag blir stadig dypere og mer komplekse, og tiltak for å gjøre disse brønnene økonomisk forsvarlig er ønsket av oljeselskapene. En metode er å redusere den ikke-produktive tiden under boring ved å analysere kroklast responsen når hindringer i brønnen oppstår. Målet er å gjenkjenne unormal adferd så tidlig som mulig for å hindre hendelser som fører til ikke-produktiv tid, for eksempel at borestrengen setter seg fast.

I denne avhandlingen har en matematisk modell for å simulere kroklast under normale tripping-forhold blitt laget. Modellen er basert på teori om krefter i borehullet, og egenskapene til borestrengen og brønnbane blir brukt. Målet er å lage gode kroklast simuleringer for enkle tripping-forhold. Hindringer i brønnen fører til problemer under tripping-operasjoner. Hvis hindringer skulle oppstå ville endringene i kroklast under tripping identifiseres raskt, og tiltak raskt settes i gang.

Et laboratorium som simulerer tripping ut av en nesten horisontal brønn er bygd og eksperimenter i den utført. Laboratorieforsøkene er utført med og uten sirkulasjon av borevæske for å identifisere de kreftene som er avhengig av sirkulasjon. Utrasing av formasjon i borehullet har og blitt etterlignet for å se hvordan hindringer påvirker kroklasten. Modellen består av matematiske formler som beskriver alle krefter pŇ borestrengen. Laboratorieresultatene brukes til å justere formlene, slik at de passer oppførselen til kroklast enda bedre.

Ved sammenligning med laboratorieresultater ble det funnet at modellen skaper nøyaktige kroklastsimuleringer under enkle forhold. Simuleringer med sirkulasjon av borevæske under tripping var unøyaktige fordi de kreftene som oppstår under sirkulasjonen var dårlig matematisk beskrevet i modellen. Det er ikke mulig å kjøre virkelig sanntidsboredata i modellen for å se om modellen er realistisk fordi posisjonsmålingene til blokka mangler, og noen målingsrater er for lave slik at formlene i modellen ikke er generelle nok. Med forbedrede posisjonsmålinger og påfølgende justeringer i modellen, er det sannsynlig at modellen for kroklastoppførsel kan brukes til å redusere ikke-produktiv tid under boring.

Contents

List of Figures

List of Tables

1 Introduction

As the drilling industry moves to deeper and more complex reservoirs, the wells get correspondingly more expensive. One action to make these wells more economically justifiable is to reduce the Non-productive time (NPT) during drilling operations. A method for early detection of restrictions in the borehole and subsequently avoid NPT is desired. Restrictions can be ledges, key seats, and poor hole cleaning among other things. It is during tripping in or out of the well that these restrictions most often become an issue. Therefore, tripping operations will be in focus throughout this report.

Hook load (HKL) is one of the parameters of the real time drilling data (RTDD) measured during drilling operations. The HKL depends on several parameters like trajectory of the well, friction between the drill string and borehole wall, density of drilling fluid and drill string and amount of cuttings, etc. The HKL can be used to detect restrictions in the well and distinguish between the causes of restriction by analysing the characteristics of the anomalies in the HKL data plot. By distinguishing between the restrictions, the correct remedies may be applied quickly, and NPT due to borehole restrictions may be minimized to a certain degree. Also ÒhiddenÓ NPT due to reaming and washing of the borehole could be minimized. This is achieved through the combination of starting reaming only when necessary and reaming appropriately, as dictated from interpretations of the HKL plot.

In order to detect anomalies in the HKL data plot, the ideal behavior of the HKL must be known. Then, the data from the well can be compared with the model and determine if the HKL data are sufficiently fitting the specific model. In this thesis, simulations of tripping out of a well during normal conditions will be conducted. A model created by (Mme, et al., 2012) for normal HKL behavior will be used as a foundation, and adjusted to fit the simulations from the laboratory. A theoretical foundation will be created in order to be able to make the necessary adjustments. Further, the model will be compared to the laboratory simulations to investigate if the hook load model is reliable.

2 Parameters affecting the Hook load

In this chapter the foundation for the model is introduced. The most important parameters affecting the hook load will be described, so a deeper physical understanding is achieved.

2.1 Definition

The hook load is the sum of all forces acting on the drill string, that are suspended in the hook (Schlumberger, 2012). These forces include the weight of the drill string in drilling fluid, mechanical and hydraulic frictional forces, possible restrictions, etc.

HKL = $\sum$ vertical components of the forces acting on the drill string attached to the hook (Mme, et al., 2012).

Measurements of the hook load are read from the tension in the deadline. The deadline is attached to the deadline anchor as seen in figure 1. The hook load is not directly read from the deadline, but is a function of the deadline tension and number of lines, n, between the sheaves (Luke and Juvkam-Wold, 1992).

$$HKL = F_{\mathrm{dl}} n \tag{1}$$

where:

- F_{dl} is the deadline tension
- n is the number of lines between the pairs of sheaves

This is a simplified equation. In reality there is some friction in the sheaves that leads to small deviations in the hook load measurements, but this effect is relatively small (Mirhaj, et al., 2010) and will therefore not be further investigated in this thesis.

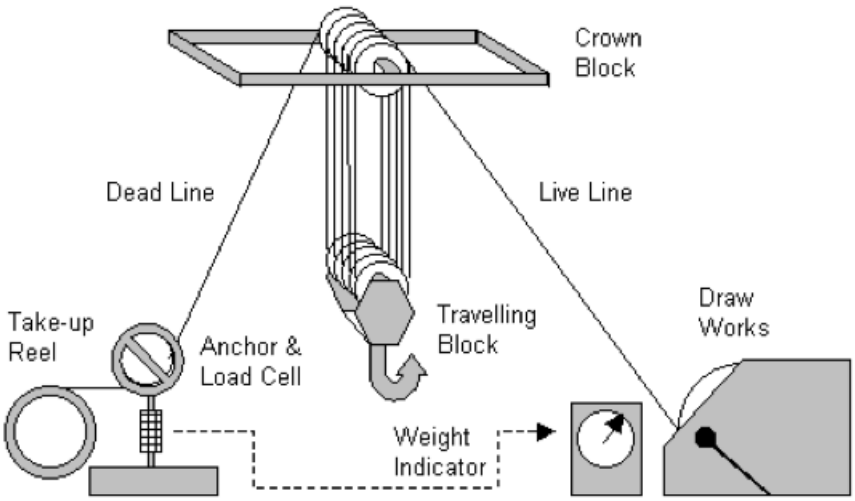

Figure 1: An overview of the hoisting system on a rig. The hook load is calculated from the tension in the deadline (Luke and Juvkam-Wold, 1992).

2.2 Drill string and mud properties

The recorded weight of the drill string suspended by the hook depends on the densities of the drill string and drilling fluid in the borehole. Figure 2 presents the forces acting on a drill string in a vertical well where the drill string is submerged in drilling fluid. There are two forces affecting the hook load in this case; gravity and buoyancy forces.

Buoyancy is the force exerted by a fluid that opposes an objects weight. In this case it is the drilling fluid that opposes the weight of the drill string. Archimedes' principle says that any object is buoyed up by a force equal to the weight of the fluid displaced by the object (Wikipedia, 2012b). Normally the net weight of a drill string component is calculated by using a buoyancy factor, for simplification. In equation 3 both gravity and buoyancy are considered.

$$\beta = 1 - \frac{\rho_{\text{mud}}}{\rho_{\text{steel}}} \tag{2}$$

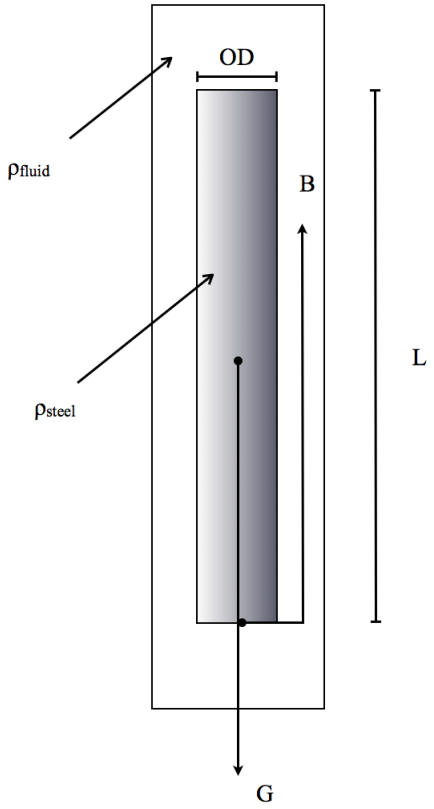

Figure 2: An illustration of the forces acting on a drill string component submerged in drilling fluid in a vertical well without any restrictions.

$$w = \rho_{\text{steel}} A_{\text{cs}} \beta g L \tag{3}$$

where

- w is the weight of drill string component in drilling fluid
- β is the buoyancy factor
- A_{cs} is the cross sectional area of drill string
- L is the length of drill string component

The viscosity of the drilling fluid, together with the velocity of the drill string also influence the hook load. When the drill string is pulled a fluidic drag is created, this will be discussed in detail later in this chapter.

2.3 Friction and side forces

Friction is defined as the force resisting the relative motion of solid surfaces or fluid layers sliding against each other (Wikipedia, 2012c). This force converts kinetic energy in to heat. The resistance to relative lateral motion between two solids is called dry friction, and is used to describe the friction force in the borehole between the drill string and borehole wall.

2.3.1 Friction

The friction force value can only be found empirically. Coulomb friction is an approximate model used to calculate the force of dry friction.

$$F_{\mathrm{f}} \leq \mu F_{\mathrm{n}} \tag{4}$$

where

- F_{f} is the force of Coulomb friction.
- μ is the coefficient of friction (COF).
- F_{n} is the normal force.

F_{f} may take any value from zero up to μF_{n}, depending on the pulling force. The direction of F_{f} is in the exact opposite direction of the relative motion between the two surfaces. When the drill string is lowered, the friction acts upwards, and when the drill string is hoisted, the friction acts downwards. Figure 3 is a simplified sketch of the forces acting in a relative motion situation.

The normal force is the component, perpendicular to the surface of contact, of the contact force exerted on an object by the surface, and prevents the object from penetrating the surface. As seen from figure 3 this normal force equals the gravity component pointing in the opposite direction of the normal force. Therefore the following equation obtains the normal force:

$$F_{\mathrm{n}} = G_{\mathrm{y}} \tag{5}$$

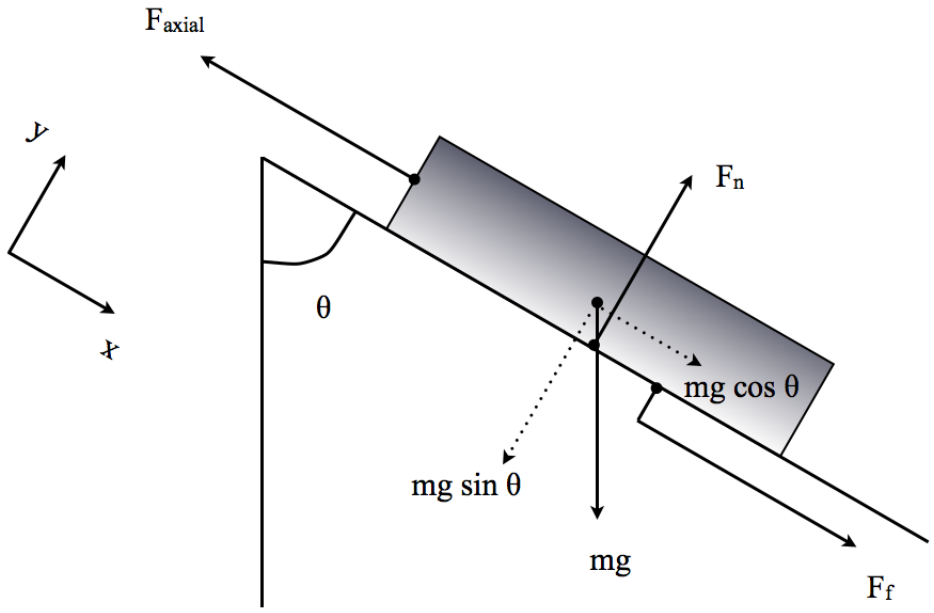

Figure 3: The forces acting on an object sliding along a solid surface. It illustrates the same forces that act between the drill string and contact surface in the borehole. F_{axial} is the force pulling on the drill string component.

$$F_{\text{n}} = mg \sin \theta \tag{6}$$

Friction forces arise whenever the drill string is in contact with the walls in the well. There is no such thing as a completely vertical well, so to some degree there is always contact between the walls and drill string. In non-vertical wells there are tangential sections and build-up and drop sections. The normal force value increases as the inclination angle increase, which can be seen from equation 6. This is a consequence of the fact that a larger part of the drill string weight rests on the borehole wall.

2.3.2 Side forces

Side forces are created in curved sections in the borehole, due to tension in the drill string. The drill string is pressed against the borehole wall as seen in figure 4, this creates an extra force between the two surfaces.

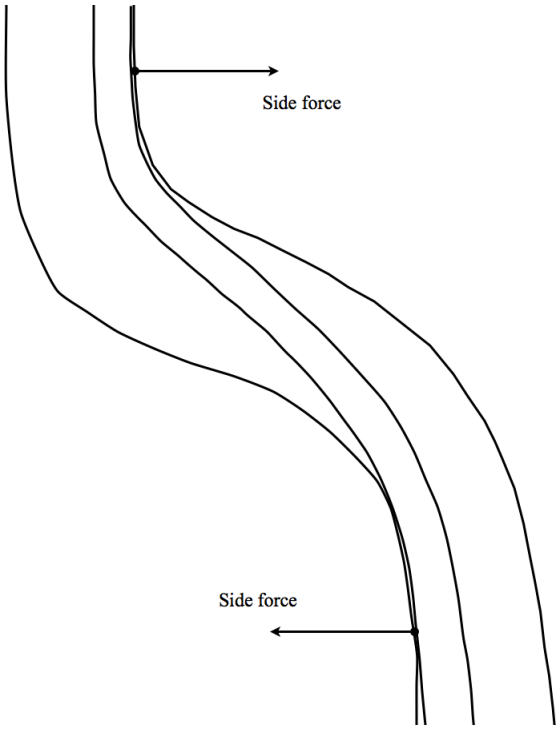

Figure 4: Side forces acting on a drill string element in tension.

2.3.3 Hydrodynamic viscous force

Hydrodynamic viscous force, also called fluidic drag force, is a drag force exerted on the drill string by the surrounding fluid in the relative direction of the fluid. When the drill string is pulled up, the drilling fluid will create a drag on the drill string in the opposite direction. Fluidic drag force is a function of relative velocity between the fluid and drill string, and the viscosity of the drilling fluid.

$$F_{\mathrm{D}} = \pi d_{\mathrm{s}} \tau L \tag{7}$$

$$\tau = \mu_{\mathrm{mud}} \frac{dv}{dy} \tag{8}$$

where

- F_{D} is the fluidic drag force
- τ is the shear stress at the surface of the pipe
- v is the relative velocity
- y is the position in the annulus between center and pipe wall.

If a constant velocity in the cross section of the annulus is assumed, then $\frac{dv}{dy}$ = 0 and equation 7 can be rewritten:

$$F_{\mathrm{D}} = \frac{\pi d_{\mathrm{s}} \mu_{\mathrm{mud}} v}{d_{\mathrm{h}} - d_{\mathrm{s}}} L \tag{9}$$

The drag force rapidly increases as the clearance between the pipe and borehole wall decreases. Assuming a constant velocity profile in the annulus cross section is a simplification and a source of error. In equation 9 it seems that the velocity and viscosity impacts the drag force equally, but in reality the viscosity of the fluid has greater impact on the drag force than the velocity (Polak and Lasheen, 2002).

With an increasing inclination angle, the effect from the hydrodynamic friction becomes less important. For the slant holes inclined more than 60 °, its contribution to the calculated borehole friction factor is small. The reason for this is that the sliding friction dominates all other effects (Maidla and Wojtanowicz, 1987).

2.3.4 Coefficient of friction

The coefficient of friction is a dimensionless scalar value, defined as the ratio of the force required to move the object and the normal force between the two surfaces (Belaskie, McCann and Leshikar, 1994). The COF is not a

function of mass or volume, but depends on the materials involved only. The dry friction is divided in two parts:

- Static friction
- Kinetic friction

Static friction is the friction between two surfaces where there is no relative motion, while kinetic friction is the friction between two surfaces where there is relative motion. Usually the COF is higher when there is no movement, and drops as soon as the surfaces move relatively to each other.

$$\mu_s > \mu_k \tag{10}$$

An applied force must overcome the static friction before an object can move. While the object is standing still, the friction force is equal to the applied force. As soon as the object starts moving, static friction is no longer applicable and the friction is called kinetic friction. This phenomena is illustrated in figure 5. It is important to separate these two situations for later when hook load will be analysed. During tripping of a stand, the drill string goes from standing still, to movement.

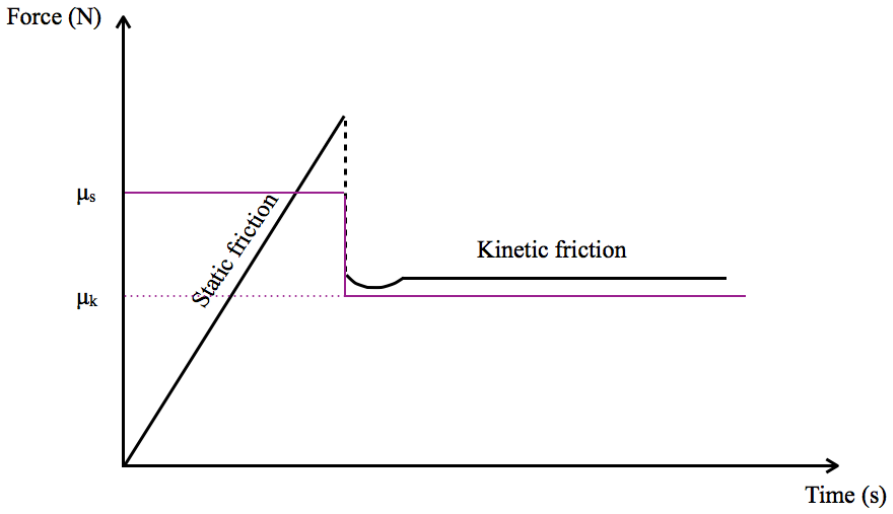

Figure 5: Ideal behavior of the Coulomb friction. The maximum point is the maximum force that the static friction can withstand. When the applied force increases above this value, the object starts sliding. The 'dump' that occurs when kinetic friction starts dominating is due to acceleration of the object.

2.3.5 Estimation of coefficient of friction

As previously mentioned, the friction must be calculated empirically, or more specific, the COF must be calculated empirically. Knowing what the material, or rock, is composed of in the entire well is not possible. Neither is knowing exactly where there is contact between the drill string and borehole wall or how large part of the drill string surface area that is in contact with the wall. Hook load is basically the weight of the drill string plus/minus friction, and an estimation of the friction factor may provide a prediction of what the hook load ideally should be. The measured hook load includes all forces working against the pipe movement, thus the COF represents all possible mechanisms working against the pipe movement in the open hole. The purpose of friction analysis is to determine whether borehole conditions are improving or deteriorating (Bible, Hedayati and Choo, 1991). An increasing friction factor suggests that restrictions are created, while a deteriorating friction factor may suggest good results from corrective actions.

Discovering restrictions at an early stage and initiate remedies before valuable time is lost, is important for the oil industry and could possibly save a lot of cost and time. Therefore several models have been developed to determine the COF in a borehole as accurate as possible. Common for most models is the use of the measured hook load from RTDD.

The model presented in (Bible, Hedayati and Choo, 1991) uses overpull and slackoff in addition to theoretical hook load to estimate the COF. Overpull is defined as the additional experienced weight to the theoretical hook load while pulling the drill string, and slackoff is defined as the measured hook load minus the theoretical hook load. Theoretical hook load is the weight of the drill string in drilling fluid, which is illustrated in figure 2.

The procedure is to create a table of expected hook loads for a range of friction coefficients at predefined depths. During tripping, the hook load measurements are used to look up the COF in the table. This is done continuously, and any suspicious behavior would be the result of unwanted situations, like accumulation of cuttings bed.

Step by step procedure:

1. Calculate the anticipated hook load for different friction coefficients for the predetermined depths by the use of the following equations:

$$HKL = \sum_{Bit}^{Surface} [w \cos\theta \pm \mu F_{\mathrm{n}}] \tag{11}$$

$$F_{\mathrm{n}} = \sqrt{(F_{\mathrm{w}} \Delta\phi \sin\theta)^2 + (w \sin\theta + F_{\mathrm{w}} \Delta\theta)^2} \tag{12}$$

where

- w is the weight of drill string element in drilling fluid
- θ is the inclination for the current component
- μ is the COF for the well
- F_{n} is the normal force
- F_{w} is the force from the bit up to the current component
- $\Delta\phi$ is azimuth change, ϕ_2 - ϕ_1
- $\Delta\theta$ is inclination change, θ_2 - θ_1

All these calculated values are defined in a COF table.

2. Measure actual hook load and find the corresponding COF from the table.
3. Continuously monitor the COF. If the COF changes rapidly, unwanted situations might be in progress in the well.

The model presented in (Maidla and Wojtanowicz, 1987) is also based on the concept that the COF is constant throughout the depth of the well and independent of the wellbore trajectory. The definition of the COF is:

$$\mu = \frac{|HKL - W \pm F_{\mathrm{D}}|}{\int^{D} F_{\mathrm{n}} \mathrm{d}L} \tag{13}$$

where

- μ is the COF for the well
- W is the weight of the drill string in drilling fluid
- F_{D} is the hydrodynamic viscous drag

– F_n is the normal forces

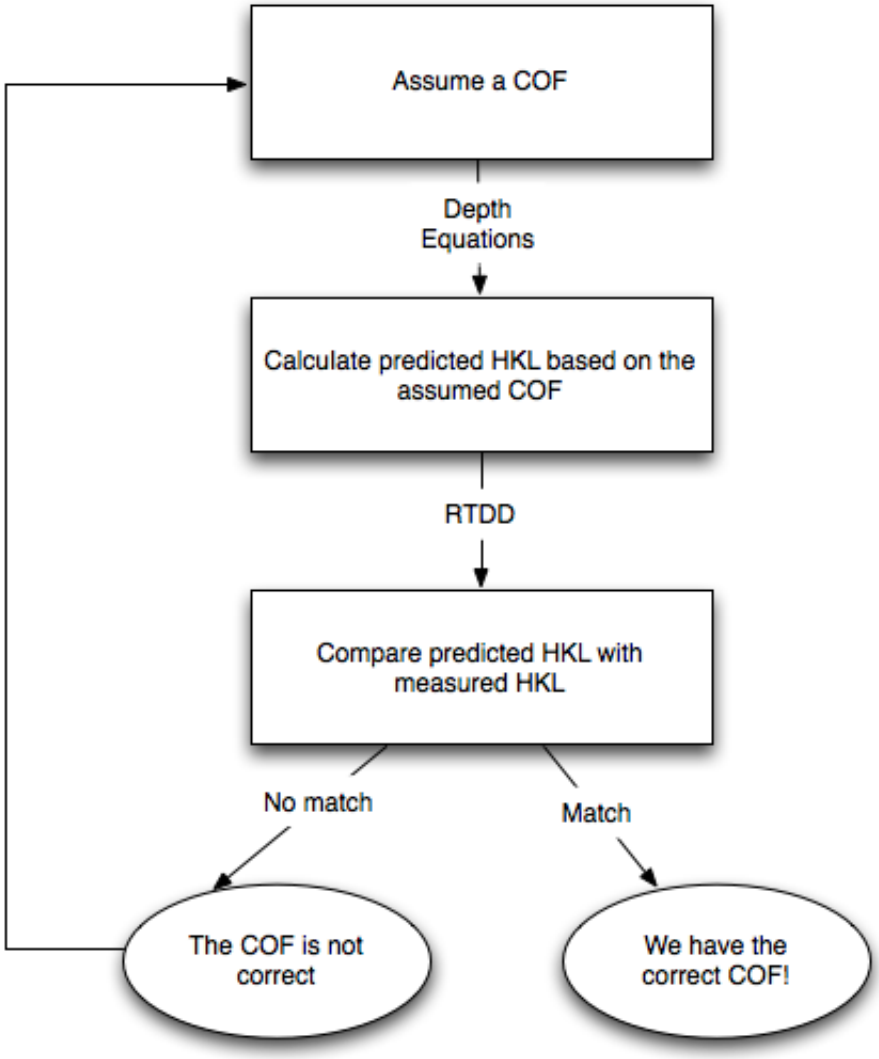

Figure 6: Flow chart of the method of finding the suitable COF in (Maidla and Wojtanowicz, 1987).

Equation 14 is used in this model, and the procedure is illustrated in figure 6.

$$HKL = F_{\text{axial}} \pm \frac{\pi}{4} \sum_{m=1}^{M} \frac{\mathrm{d}p}{\mathrm{d}l} L {d_{\text{s}}}^2 \tag{14}$$

The second term in equation 14 accounts for hydrodynamic friction effects. The analysis of the results from this model concluded that the hydrodynamic effects become less important with increasing inclination angle. For the slant holes inclined more than 60 ° the contribution from the hydrodynamic forces to the calculated value of the COF was smaller than 17 %. The reason for this phenomenon is that in high-inclination holes, the sliding friction dominates all other effects, particularly the effect from the swab and surge pressures, which by their nature are independent from the inclination angle.

What mainly separates the two discussed models is the consideration of the hydrodynamic viscous drag. The first model does not include this part while calculating the hook load, thus making fluidic drag one of the mechanisms influencing the COF. Otherwise, they have similar approach; assume a COF and compare to measured hook load until they match.

2.4 Wellbore geometry and restrictions

One single value for an overall friction factor represents all possible mechanisms working against the drill string pipe movement in the open hole. Examples of these mechanisms are:

- Cuttings bed
- Dog legs
- Key seats
- Ledges
- Washouts
- Swelling shale

Hook load depends largely on the trajectory of the well. Inclination affects both the experienced weight and normal force as seen from the following equation:

$$F_{\text{axial},2} = F_{\text{axial},1} + w\cos\theta \pm \mu F_{\text{n}} \tag{15}$$

Equation 15 is derived from figure 3, and is another way of writing equation 11. $F_{\text{axial},2}$ is the force needed to pull the current drill string component plus the drill string components beneath the current one. From these equations it can be seen that the experienced weight decreases, while the normal force increases with increasing inclination, θ.

Cuttings bed is a problem arising in deviated wells, where the settling distance is reduced drastically compared to vertical wells. The vertical velocity component is also reduced, so the drilling fluids capability to keep cuttings in suspension is decreased (Skalle, 2010). In vertical wells the cuttings are able to stay suspended in the drilling fluid even when circulation stops, but in deviated wells the cuttings settle on the lower borehole wall as seen in figure 7. Once the cuttings settle, it is difficult for the drilling fluid to suspend the cuttings again due to low fluid velocity near the borehole wall. The concentration of cuttings in the well increase, and beds are created. Problems related to these cuttings bed mostly arise during tripping or back reaming. During pulling of the drill string, the beds are dragged along with the drill string causing cuttings accumulation around the string. An increase in hook load follows. If this restriction is discovered in time, stuck pipe might be avoided.

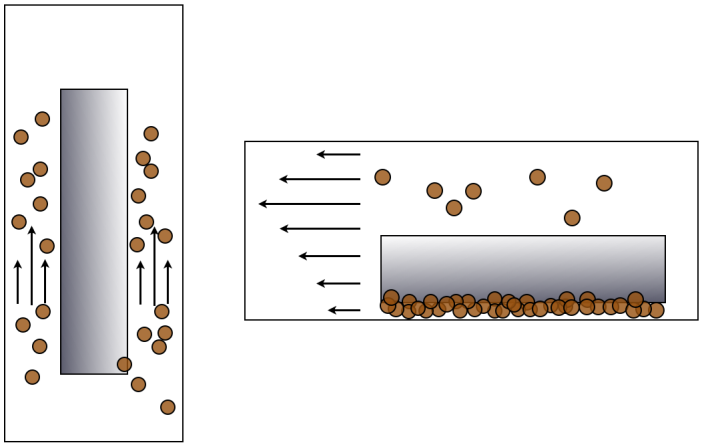

Figure 7: The brown circles illustrate cuttings in the well, and the arrows indicate the drilling fluid velocity in the annulus. Note how the cuttings accumulate underneath the horizontal drill string element.

Dogleg is the term used for areas in the wellbore where the trajectory rapidly changes direction. The dogleg is sometimes planned by the driller, but the term can also be used for sections where the direction changes faster than anticipated or desired (Aadnoy, et al., 2009). High doglegs may create problems like key seating or drill string fatigue, thus causing an increase in torque and hook load.

In a dogleg section, the drill string is in contact with the side of the wall. During drilling the pipe will gradually wear away a small-diameter groove slot in the side of the borehole wall (Aadnoy, et al., 2009). The cross section at this point shows that the hole now is slightly formed as a 'keyseat' as seen in figure 8. When the drill string is pulled or lowered in the well, these key seats may become a problem. Tool joints, drill collars and other drill string equipment where the drill string diameter increase could get stuck in key seat sections. The pipe slides through the key seat, but as the diameter increase, the drill string gets stuck. Ledges can be seen as erratic changes in the hook load measurements, and may in worst-case lead to stuck pipe. Ledges are created where the formation alternate between soft and hard rock, and are similar to key seats when it comes to restriction problems.

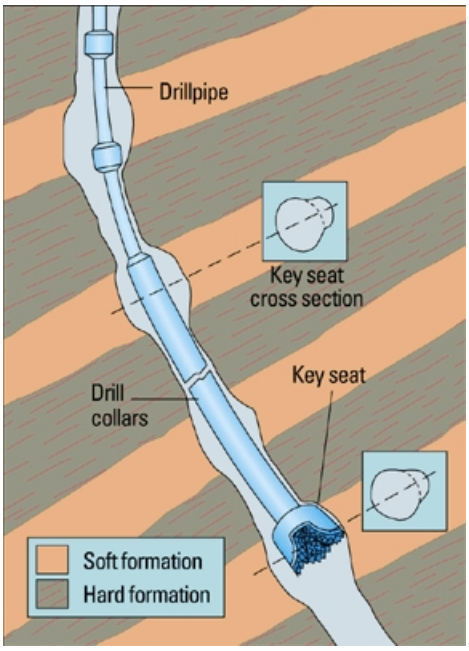

Figure 8: An illustration of how key seats are formed (Oilfield Glossary, 2012).

Common for all of these problems are that they influence the hook load to some degree. And some of them occur more frequently in deviated sections than in vertical sections. By monitoring the trend of hook load, or COF, it is believed that the NPT caused by these restrictions could be reduced. The restrictions will appear as changes in the hook load, and they are important to identify in order to use correct remedies.

2.5 Elastic properties and inertia forces

2.5.1 Elastic properties

The drill string is composed of steel, which is an elastic material. Due to this characteristic, the drill string behaves in a certain way that affects the hook load measurements. This behavior must be taken into account when the hook load model is created.

An elastic modulus is a mathematical description of the elasticity of a specific material. The modulus describes the ability of the material to elastically deform when it is subjected to a force. This elastic deformation is not permanent. When the force ceases the material goes back to its original form. The definition of elastic modulus is the slope of the material's stress - strain curve in the elastic deformation region. Thus, a higher modulus means a stiffer material.

$$\lambda = \frac{stress}{strain} = \frac{\sigma}{\varepsilon} \tag{16}$$

$$\sigma = \frac{F}{A_{\text{cs}}} \tag{17}$$

$$\varepsilon = \frac{l - L}{L} \tag{18}$$

where λ is the elastic modulus. F is the force applied on the material, L is the initial length of the object and l is the final length of the object.

There are several types of elastic moduli, and for the forces applied on the drill string, the Young's modulus applies. Young's modulus describes the

tensile elasticity of the drill string, meaning the drill string's tendency to deform along its axis. Equation 16 gives the behavior of the drill string in tension and shows that the elasticity is linear. This behavior is generalized in Hooke's law, which says that the extension of a spring is proportional to the load applied to it.

$$F = -kx \tag{19}$$

where x is the stretched distance of the spring from its equilibrium position, F is the restoring force exerted by the spring and k is a constant called the spring constant. The linear behavior of elastic materials is demonstrated in figure 9.

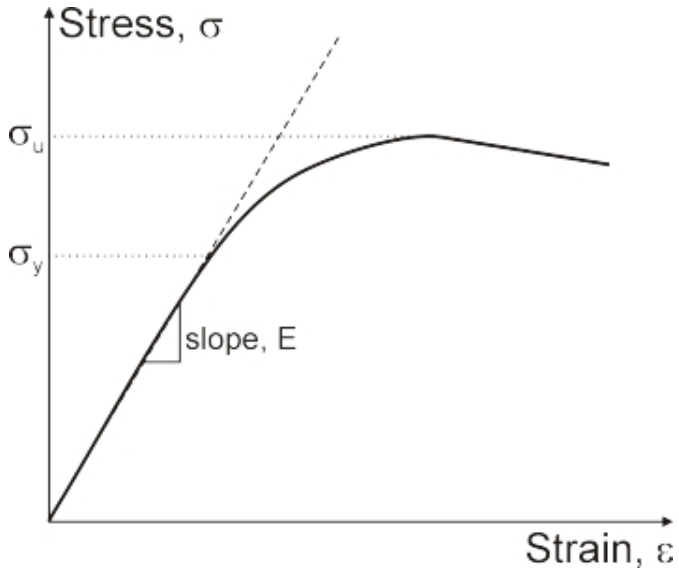

Figure 9: Linear behavior of elastic materials. The material follows Hooke's law until the stress reach the value of σ_y. When the material is subjected to higher stresses, the material will deform permanently (Massarelli, 2012).

Since the drill string follows Hooke's law until a certain applied force, the drill string can be considered as a mass-spring system in order to mathematically explain some of the physical events happening during tripping. This will be further investigated in the next chapter.

2.5.2 Inertia forces

Inertia is defined as the resistance of any physical object to change its state of motion or rest. When tripping starts, the drill string is accelerated. The acceleration causes an increase in the dead line tension, which again directly increases the hook load. This behavior is explained mathematically by Newton's second law:

$$F = ma \tag{20}$$

F is the applied force on the object, in this case the hook load pulling the drill string. Acceleration, a, is proportional to the applied force. The larger the force is, the more will an object accelerate. Mass, m, is the inertia, which is the reluctance to accelerate. For the same applied force, more massive objects experience smaller acceleration than less massive ones.

During tripping it may be difficult to maintain a constant block velocity due to constantly changing conditions in the borehole. The friction in the well changes constantly, thus affecting both the experienced weight and acceleration of the drill string. Also the elasticity may disturb the measured hook load, delaying the effects of changes in friction factor. The exact cause of variations in hook load is therefore difficult to determine.

3 Previous work

The model presented in this thesis will be based on tripping out simulations carried out in the laboratory and on the work presented in (Mme, et al., 2012). It is during tripping most of the restrictions cause trouble and stuck pipe incidents occur.

In the paper 'Analysis and modeling of normal hook load response during tripping operations', a model of hook load response during tripping is presented based on a field case study. The objective of the paper was to create a trustworthy model that matches hook load during tripping. Thus, making it possible to detect deviatory behavior early during tripping operations.

3.1 Mass-spring system

The model is developed as a mass-spring system in the paper. The components of the drill string are connected to the hook via spring elements, which represent the elasticity of the drill string. The system contains n drill string elements. The forces required for the elements to be in motion are defined by the following equations:

$$m_1 a_1 = k_{12}(x_2 - x_1 - \Delta_{1\text{-}2}) - F_{\text{f1}} - F_{\text{D1}} \tag{21}$$

$$m_2 a_2 = k_{23}(x_3 - x_2 - \Delta_{2\text{-}3}) - k_{12}(x_2 - x_1 - \Delta_{1\text{-}2}) - F_{\text{f2}} - F_{\text{D2}} \tag{22}$$

$$m_3 a_3 = HKL - k_{23}(x_3 - x_2 - \Delta_{2\text{-}3}) - F_{\text{f3}} - F_{\text{D3}} \tag{23}$$

where

- m_{n} is the mass of the drill string element n
- a_{n} is the acceleration of the drill string element n
- k is the spring constant
- x_{n} is the position of the drill string element n

- $\Delta_{\text{n-(n+1)}}$ is the initial distance between elements n and $n+1$
- F_{fn} is the frictional force for the nth element

$$F_{\text{fn}} = \beta g m_{\text{n}} \mu \sin\theta \tag{24}$$

- F_{Dn} is the fluidic drag force for the nth element

$$F_{\text{Dn}} = \frac{\pi d_{\text{s}} \mu_{\text{mud}} v}{d_{\text{h}} - d_{\text{s}}} L \tag{25}$$

Equation 21 calculates the force needed to set the bottom drill string element in motion and equation 23 calculates the force for the upper most drill string element, which is the element attached to the hook. Equation 22 is used for all other drill string elements in between. An illustration of the mass-spring system and derivation of equations 21 to 23 is presented in chapter 4, where the mathematical model in this thesis is presented.

3.2 Tripping of one stand

Tripping of a stand has been simulated in Matlab using the above equations (some simplifications have been made), and with RTDD from the field case study as input parameters. The input parameters are shown in table 1. Δ is the distance between two neighboring elements.

Table 1: Model input data (Mme, et al., 2012)

Parameter	*Value or Range*	*Unit*
Mud weight	1400	kg/m^3
Mud viscosity	0.01	Pas
Steel density	7850	kg/m^3
Mass of BHA	200	kg/m
Mass of drill pipe	30	kg/m
$\Delta_{1\text{-}2}$	76	m
Average static coefficient of friction	0.50	-
Average kinetic coefficient of friction	0.23	-
Buoyancy factor	0.82	-

In figure 10, typical behavior of hook load during tripping out of one stand without any restrictions is shown. The block position (BPOS) is plotted in the same figure in order to better interpret the course of events. The course of events is briefly described in the paper (Mme, et al., 2012).

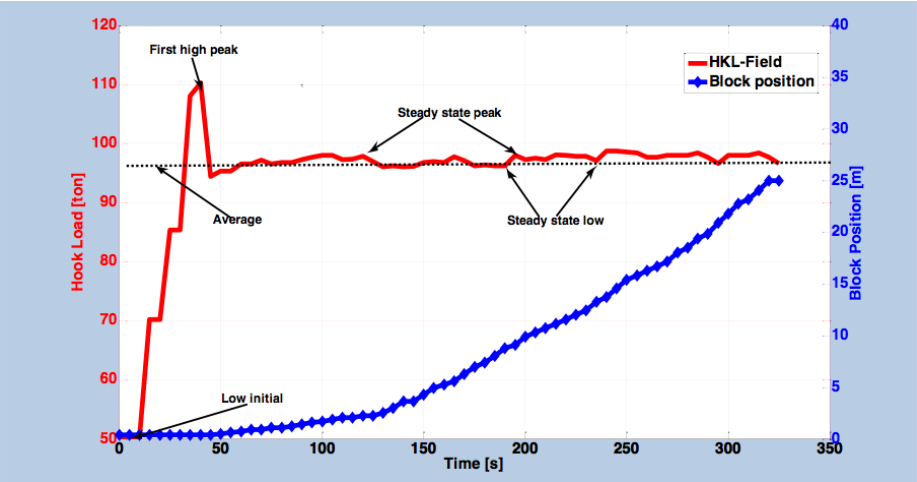

Figure 10: Normal hook load behavior during puling of one stand (Mme, et al., 2012).

Low initial is the hook load value when the block does not move. It is the weight of the drill string and block itself.

As the block starts pulling the drill string upwards, the hook load rapidly increases due to static friction.

First high peak is typically the highest hook load value during tripping out. Static friction coefficient is normally higher than kinetic friction coefficient, thus a higher force is needed to set the drill string in to motion than keeping it in motion. The shear stress increases as the drill string starts to move, leading to higher fluid friction. Also, if the circulation has been stopped for a while prior to pulling the string, gel strength may have been developed.

Steady state peak and steady state low are the small fluctuations from the average hook load value while pulling the string. After the first high peak, kinetic friction dominates, and the hook load value decreases to the average value. The fluctuations are caused by varying coefficient of friction and varying conditions in the well. Also, the flexibility of the

pipe and BHA, which encounters differing forces as the drill string is tripped out of the hole may cause fluctuations.

A value lower than the average value right after the first high peak is observed in figure 10. In addition to going from static friction to kinetic friction, the drill string experiences acceleration (not block acceleration), thus decreasing the tension in the dead line. This results in an immediate low value after the pipe movement starts.

As mentioned earlier, it is difficult to keep a constant velocity for the block due to varying conditions in the well. By comparing the acceleration of the block and the hook load, a correlation between the two is observed. This is seen in figure 11.

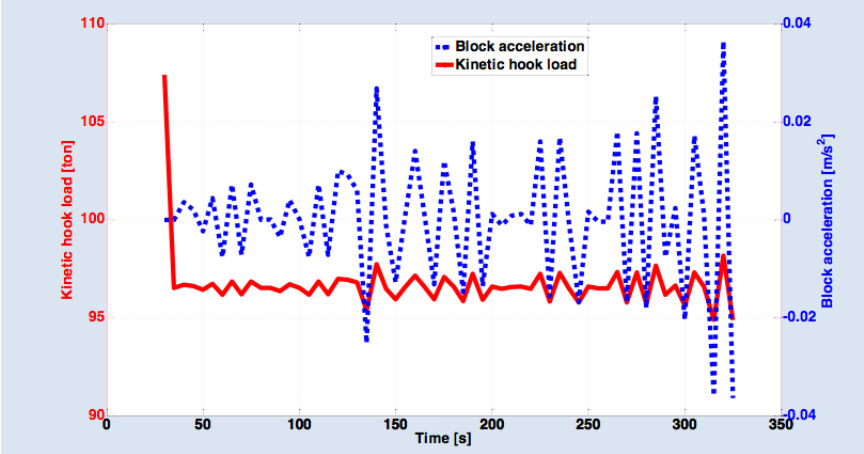

Figure 11: Observed correlation between the hook load and block acceleration (Mme, et al., 2012). The hook load increase as the block accelerates, and decrease as the block acceleration decrease.

4 Mathematical model during tripping out

The model presented in this thesis will be tested against experimental results. Some assumptions are made, and they will be presented here. The acceleration is calculated on basis of block and drill string movement in a certain time interval.

$$a = \frac{\Delta v}{\Delta t} = \frac{\Delta^2 x}{\Delta t^2} \tag{26}$$

x denotes the position of the drill string elements.

The mass-spring model presented by Mme, et al. (2012) forms the foundation for elasticity calculations. In reality a drill string experiences varying stresses along the annulus, and it is convenient to divide the string into several elements. Force calculations are made for each element at every time step t. The cross sectional area varies for both the annulus, and for the drill string. The higher the number of elements, the higher the accuracy of the model. However, the more elements in the model, the longer computation time for the Matlab simulation. The same applies for the time interval.

In the model, the BHA will act as one element, and the rest of the drill string is divided into nine elements. This gives a total of ten elements, $N = 10$, in the model. The number of elements is a balance between computation time and calculation accuracy.

The mass-spring model is presented in figure 12. The figure shows the mass-spring system with respect to time. The upper drill string has initial conditions (at time t =1), and the lower drill string has moved til time t. The drill string is pulled to the right, while fluid friction and Coulomb friction act the opposite way. The equations described in the previous chapter (equations 21 to 23) will be deducted based on this figure, to obtain a better understanding of the mass-spring model.

The forces acting on element n are fluid friction, Coulomb friction and spring force, latter on both ends. The force, F_{spring}, applied by the springs is equal to the spring constant, k, multiplied with the extension of the spring. The extension of the spring equals current distance between two elements minus the initial distance between the two same elements.

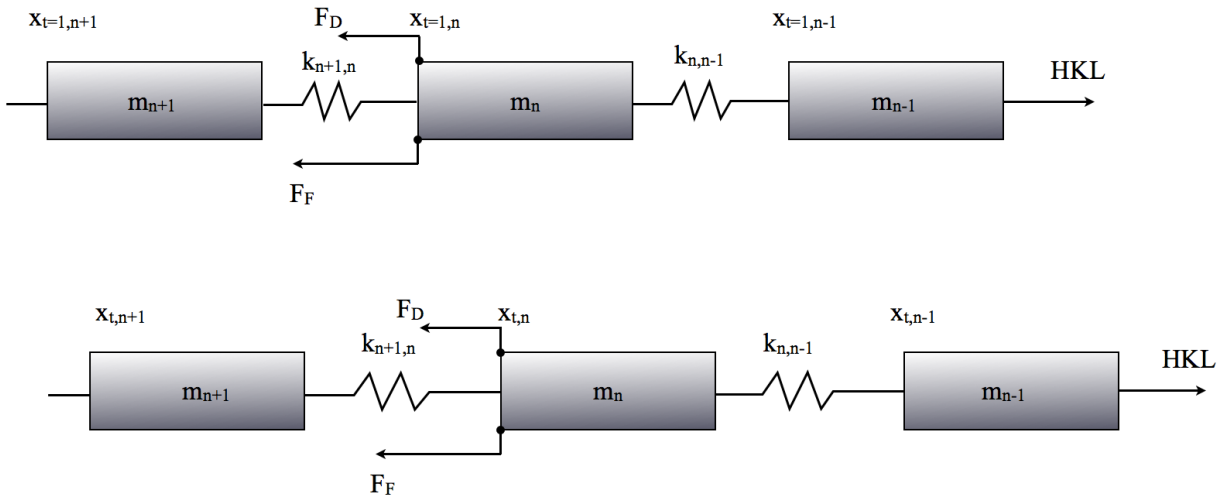

Figure 12: The mass-spring system. Above at initial time, below at time step t.

In figure 12 the initial element positions are denoted $x_{t=1,n}$, and current positions are denoted $x_{t,n}$. The spring force acting on the right side of element n, with spring constant $k_{n,n-1}$, is:

$$F_{\text{spring}} = k_{n,n-1}(x_{t,n} - x_{t,n-1} - (x_{1,n} - x_{1,n-1})) \tag{27}$$

$$x_{1,n} - x_{1,n-1} = \Delta_{n,n-1} \tag{28}$$

$$F_{\text{spring}} = k_{n,n-1}(x_n - x_{n-1} - \Delta_{n,n-1}) \tag{29}$$

The term multiplied with the spring constant in equation 29 is the extension of the spring. $\Delta_{n,n-1}$ denotes the initial distance between the two elements n and $n-1$. The same is valid for the spring with spring constant $k_{n+1,n}$. It acts in the opposite direction on element n.

The forces acting on element n are:

$$\sum F = m_n a_n \tag{30}$$

$$m_{\mathrm{n}}a_{\mathrm{n}} = k_{\mathrm{n,n+1}}(x_{\mathrm{n+1}} - x_{\mathrm{n}} - \Delta_{\mathrm{n,n+1}}) - k_{\mathrm{n\text{-}1,n}}(x_{\mathrm{n}} - x_{\mathrm{n\text{-}1}} - \Delta_{\mathrm{n\text{-}1,n}}) - F_{\mathrm{R,n}} - F_{\mathrm{D,n}} \quad (31)$$

The effect of the drill string elasticity is a combination of the acceleration of the drill string and acceleration of the block, causing changes in the dead line tension where the hook load is measured. When the pipe stretches the tension increases, and when the pipe contracts again the tension rapidly decreases. Measuring the stretch for each element in the laboratory would be difficult. Therefore the elasticity effect is created by the use of a spring attached at the upper end of the string (figure 14 in chapter 5).

$$F_{\mathrm{spring}} = k\Delta x \quad (32)$$

where F_{spring} is the force of the spring, k is the spring constant, and Δx is the extension of the spring. Δx is calculated based on the acceleration found from the laboratory drill string position data. Negative drill string acceleration means that the spring stretches, thus increasing the hook load. Positive acceleration gives decreasing hook load.

The arrangement in the laboratory is simple compared to field conditions. Some simplifications are:

- Constant inclination (84 °)
- No azimuth change
- The velocity profile of the mud in the cross section of the annulus is flat

$$v_{\mathrm{mud}} = \frac{q_{\mathrm{pump}}}{A_{\mathrm{cs}}} \quad (33)$$

- No cuttings in the system
- Water is used for circulation. Mud properties, like gelling, doesn't need consideration

Due to these simplifications many variables remain constant and few forces need to be considered. No side forces or sudden changes in annulus geometry

are included. The friction factor is however difficult to calculate, because it normally includes many unpredictable variables. In the model, the friction coefficient will be adjusted by comparing model hook load with laboratory hook load under the simplest conditions. Hopefully, an accurate and realistic estimate of the friction is achieved.

The fluidic drag force is almost fifty times larger for the BHA than for the drill pipe, for a given length interval (The derivation of this statement is presented later in chapter 6). The relative velocity between mud flow and drill string also influences the difference, but this difference gives much lower impact. The velocity of the mud increases as the cross sectional area of the annulus decreases, as seen in equation 34 for relative velocity. For the simplicity of the model, fluidic drag will only be calculated for the BHA.

$$v = v_{\mathrm{ds}} - v_{\mathrm{mud}} = v_{\mathrm{ds}} - \frac{q_{\mathrm{pump}}}{A_{\mathrm{cs}}} \tag{34}$$

The model will mainly simulate normal conditions, but the impact of washouts will also be studied. Taking all considerations mentioned in this chapter into account, the equation for hook load becomes:

$$HKL(t) = F_{\mathrm{weight}} + F_{\mathrm{spring}}(t) + \sum_{n=1}^{N} F_{\mathrm{f}}(t,n) + F_{\mathrm{D,BHA}}(t) \tag{35}$$

This equation will be used in the Matlab simulations. $\mathrm{F_f}$ is the friction force, and it is the only force that varies for each element at time, t.

It is important, however, to check that the conditions for movement of drill string are fulfilled. The forces must overcome the static friction if the drill string has not moved previously. The static friction coefficient will be set experimentally.

5 Tripping out experiments

A laboratory experiment has been built and set up for the purpose of simulating pulling of a drill string during tripping out. The drill string position and the force used to pull the drill string are measured with a given sampling rate. A plot of hook load and drill string position vs. time can then be made. The drill string position is the distance the drill string has been pulled from starting point zero. It is possible to adjust the block velocity, to circulate drilling fluid during tripping, and to simulate wellbore washouts of different sizes.

The laboratory experiments are performed to obtain a better understanding of the impact on hook load for different parameters. Functions or models for these parameters will then be created in Matlab code so an estimation or prediction of the hook load is found.

5.1 The Laboratory set up

The laboratory consists of a 5,9 meter long drill string, including BHA, which is attached to a spring. The spring is attached to a force indicator, which again is attached to the 'hook'. The whole arrangement has smaller dimensions than in the field, and are shown in figure 13 and 14.

The dimensions of the laboratory equipment have been measured manually, and are listed in table 2.

Table 2: Laboratory dimensions

Equipment	*Value*	*Unit*
BHA diameter	49	mm
Drill string diameter	10	mm
Inclination angle	84°	
Length of BHA	0,93	m
Length of drill string	5	m
Total length of laboratory set up	12	m
Spring constant (k)	2730	N/m

Note that the inclination angle is described as deviation from vertical direc-

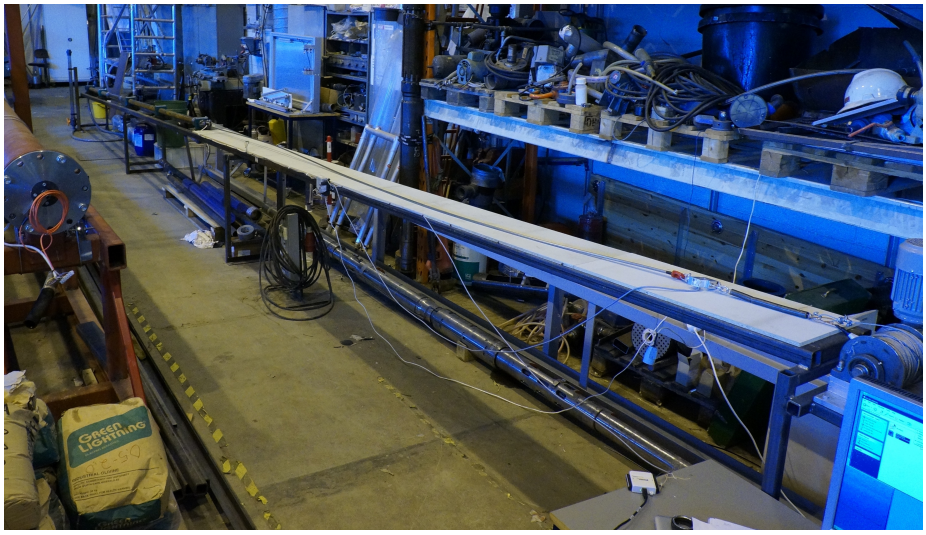

Figure 13: An overview of the laboratory set up. In this picture, the drill string has been pulled out of the annulus.

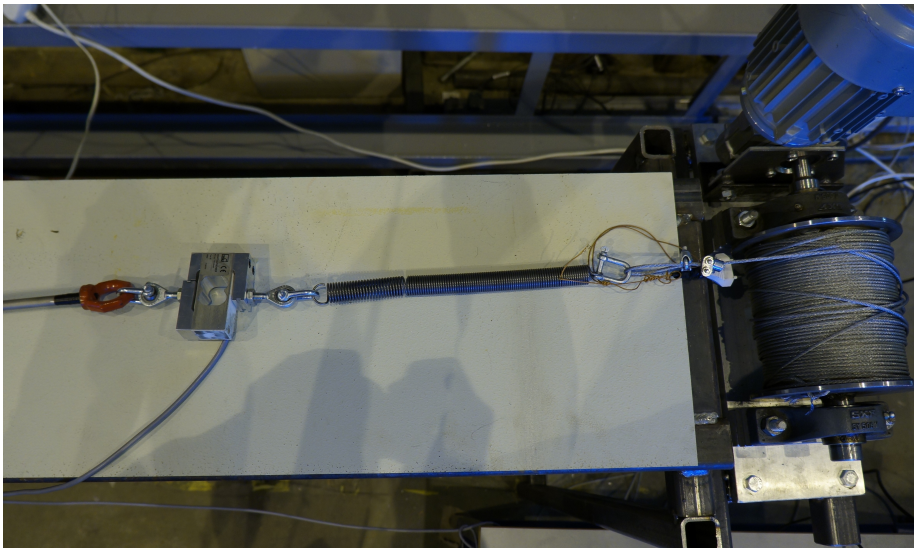

Figure 14: A closer view at the 'hook'. The drill string (left) is connected to the pulling wire (right) via a spring (middle) where the pulling force is measured.

tion. In figure 15, a sketch with dimensions and laboratory equipment is presented.

In figure 13 the drill string is pulled out of the annulus, while the BHA

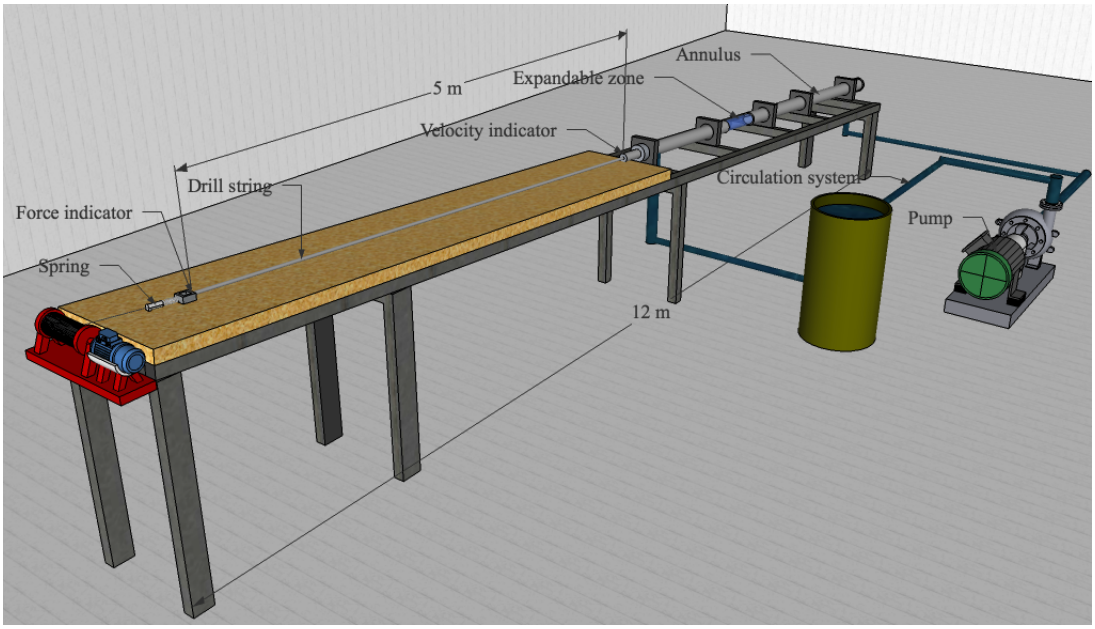

Figure 15: A sketch of the laboratory experiment to illustrate important devices. The wellbore is inclining 84 °.

is remained in the annulus. In the laboratory the BHA cannot be pulled out from the wellbore pipe. During simulations, the complete drill string is initially inside the annulus. Block velocity is defined by setting a frequency for the pulling motor, and the wire starts pulling (tripping out) the drill string while drill string position and force are measured and collected in a Labview program designed by Uduak Mme. The device measuring the force is seen in figure 14, where it is placed between the spring and the drill string. The position is measured by using a reel, as seen in figure 16. After pulling 4,9 m (the length of the drill string), the motor is manually stopped, and tripping is completed. There is an automatic disconnection in case of emergencies (if the drill string is not stopped in time, the BHA will slam into the annulus exit). Note that the measured position is not the block position, but the distance the drill string has travelled. For stiff arrangements these values should be the same, but stretching of the spring causes a difference, which accounts for the elasticity.

As mentioned, it is possible to circulate drilling fluid in the annulus. The thin pipes, connected to the annulus in figure 15 are used for circulation (marked 'circulation system'). The pump sucks drilling fluid from the cylin-

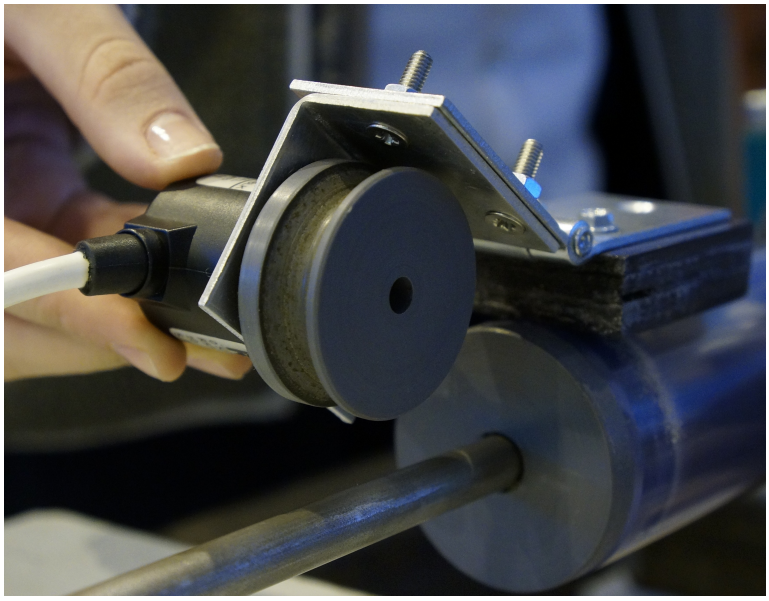

Figure 16: The diameter of the reel is 10 cm. For every revolution the reel sends 500 pulses to Labview. In this way, the drill string position and velocity of the drill string can be calculated.

drical bucket, and pumps it into the annulus at the rear end. The fluid flows through the drill string and BHA annulus, out through the thin pipe underneath the foremost end of the annulus, and back into the bucket. The maximum pump rate is approximately 37 L/min (0,000617 m^3/s), predicting a maximum velocity in the open wellbore of 0,264 m/s.

Washout is simulated by substituting a part of the annulus with a pipe that has larger diameter, as seen in figure 17. The length of the washout may also vary.

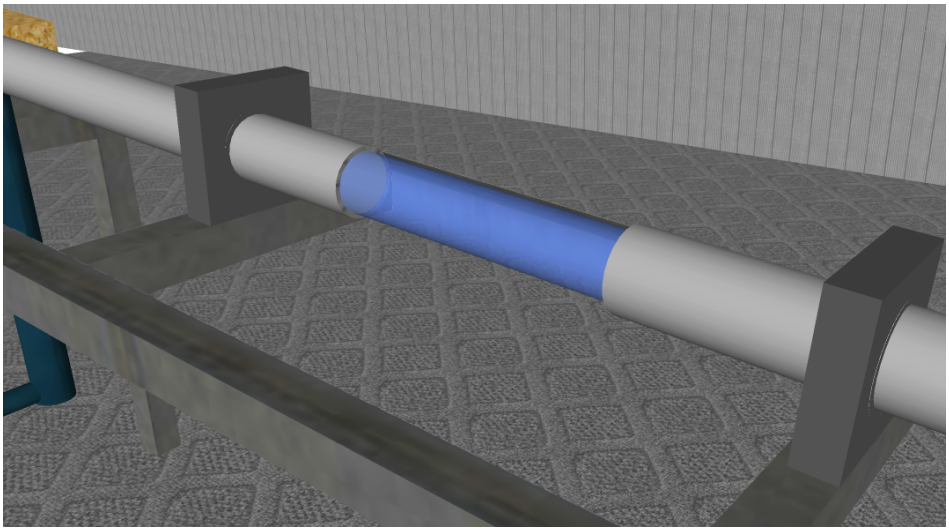

Figure 17: The plexi pipe in the middle of the wellbore length, can be replaced with other pipes with larger diameter in various lengths to imitate formation washouts.

The input parameters to the hook load model are collected and listed in table 3. The mud is simply water (at 20 °C) and the material used in the laboratory is structural steel, which is very common.

Table 3: Input data from the laboratory. Mass and buoyancy factor are calculated on basis of the other parameters in the table.

Parameter	*Value or Range*	*Unit*
Mud weight	1000	kg/m^3
Mud viscosity	0,001	Pas
Steel density	7850	kg/m^3
Initial traveling block position	0	m
Mass of BHA	15,41	kg/m
Mass of drill pipe	0,62	kg/m
Buoyancy factor	0,873	-

In the laboratory, some of the equipment are not in proportion with each other. For example, the BHA has an outer diameter that is five times larger than the outer diameter of the drill string (table 2). If these were real proportion, the BHA would be 25 inches in diameter while using normal 5 inch drill pipes. Because of this huge difference in diameters, it could be assumed that a large part of the exerted forces in the annulus is exerted on the BHA.

Take for instance fluidic drag. The clearance in the annulus is known, so the fluidic drag force for the BHA element and drill string elements can be compared:

$$F_{\mathrm{D}} = \frac{d_{\mathrm{s}}}{d_{\mathrm{h}} - d_{\mathrm{s}}} \pi \mu_{\mathrm{mud}} v L \tag{36}$$

$$\frac{F_{\mathrm{D,BHA}}}{F_{\mathrm{D,drill\ string}}} = \frac{\frac{OD_{\mathrm{BHA}}}{ID_{\mathrm{annulus}} - OD_{\mathrm{BHA}}}}{\frac{OD_{\mathrm{drill\ string}}}{ID_{\mathrm{annulus}} - OD_{\mathrm{drill\ string}}}} = \frac{\frac{0{,}05}{0.0545 - 0{,}05}}{\frac{0{,}01}{0{,}0545 - 0{,}01}} = 49,4 \tag{37}$$

The fluidic drag force is almost fifty times larger for the BHA element than for the drill string elements. Due to these abnormal proportions there may arise other 'problems' that normally are not an issue, and these must be taken into consideration as the experiments are carried out.

5.2 Test matrix

A test matrix for the laboratory experiments conducted in this thesis has been created in order to obtain a good overview, see table 4. Mme, et al. (2012) has created a test matrix that includes the tests that will be carried out in this thesis. In addition, it includes testing with other parameters, such as cuttings in the annulus. The test matrix presented in table 4 is derived from that matrix.

In the case of no expansion, a pipe with a slightly smaller diameter than the annulus is used, see figure 17. The ID is 52 mm while the annulus has ID 54,5 mm. The diameter of the BHA is 49 mm, and the decrease in annulus clearance in this zone must be taken into consideration. In the test matrix, two different expansion selections are used. They are described in table 5.

Table 4: Test matrix. A frequaency of 20 Hz gives a pulling velocity of approximately 0,12 m/s.

Test	*Frequency*	*Expansion*	*Circulation*
1	20 Hz	none	none
2	40 Hz	none	none
3	60 Hz	none	none
4	20 Hz	none	x
5	40 Hz	none	x
6	60 Hz	none	x
7	20 Hz	1	none
8	40 Hz	1	none
9	60 Hz	1	none
10	20 Hz	1	x
11	40 Hz	1	x
12	60 Hz	1	x
13	20 Hz	2	none
14	40 Hz	2	none
15	60 Hz	2	none
16	20 Hz	2	x
17	40 Hz	2	x
18	60 Hz	2	x

Table 5: Expansion selections

Expansion number	*ID*	*OD*	*Length*
1	82 mm	90 mm	20 cm
2	82 mm	90 mm	96 cm

5.3 Laboratory results

In this section, results from the laboratory test matrix (chapter 5.2) will be presented. Graphs will be explained and compared with each other. For each laboratory test an excel file is created through Labview, containing the hook load signal and the drill string position. Hook load is measured 1000 times per second, while position is given once per second. From this file the velocity and acceleration of the drill string are calculated.

5.3.1 Initial conditions

The first three tests in the test matrix are the simplest ones, where there are no fluidic drag or wash out effects affecting the hook load. There is no circulation, and no expansions are installed. The results are shown in figures 18 to 20 (two plots for each hook load simulation, one for each sampling rate). Upper plot in figure 18 shows hook load and position vs. time (one measurement per second) and the lower plot shows hook load vs. time with 1000 measurements per second, and velocity vs. time with one measurement per second. The motor frequencies 20, 40 and 60 Hz is referred to as low, medium and high pulling velocity respectively.

The model will use the position measurements as input for the simulations, thus the hook load sampling rate will be once per second also. Therefore, the hook load plots with one measurement per seconds are presented in addition to the plots with 1000 measurements per second, in order to create a good basis for the comparison of laboratory experiments and simulation results.

The lower plot in figure 18 is a good example of how the hook load performs during experiments. The average value is about 140 N, with steady state fluctuations. There is no "First high peak" in the laboratory measurements, since the mass and friction forces are too low. The proportions of the laboratory equipment are different from real wells, and the well is nearly horizontal. The weight of the drill string is low, compared to how strong the pulling motor is.

The hook load responds to block acceleration, a correlation which was presented in figure 11. The optimal way of interpreting the experimental results would be to display these two parameters together, to study the correlation.

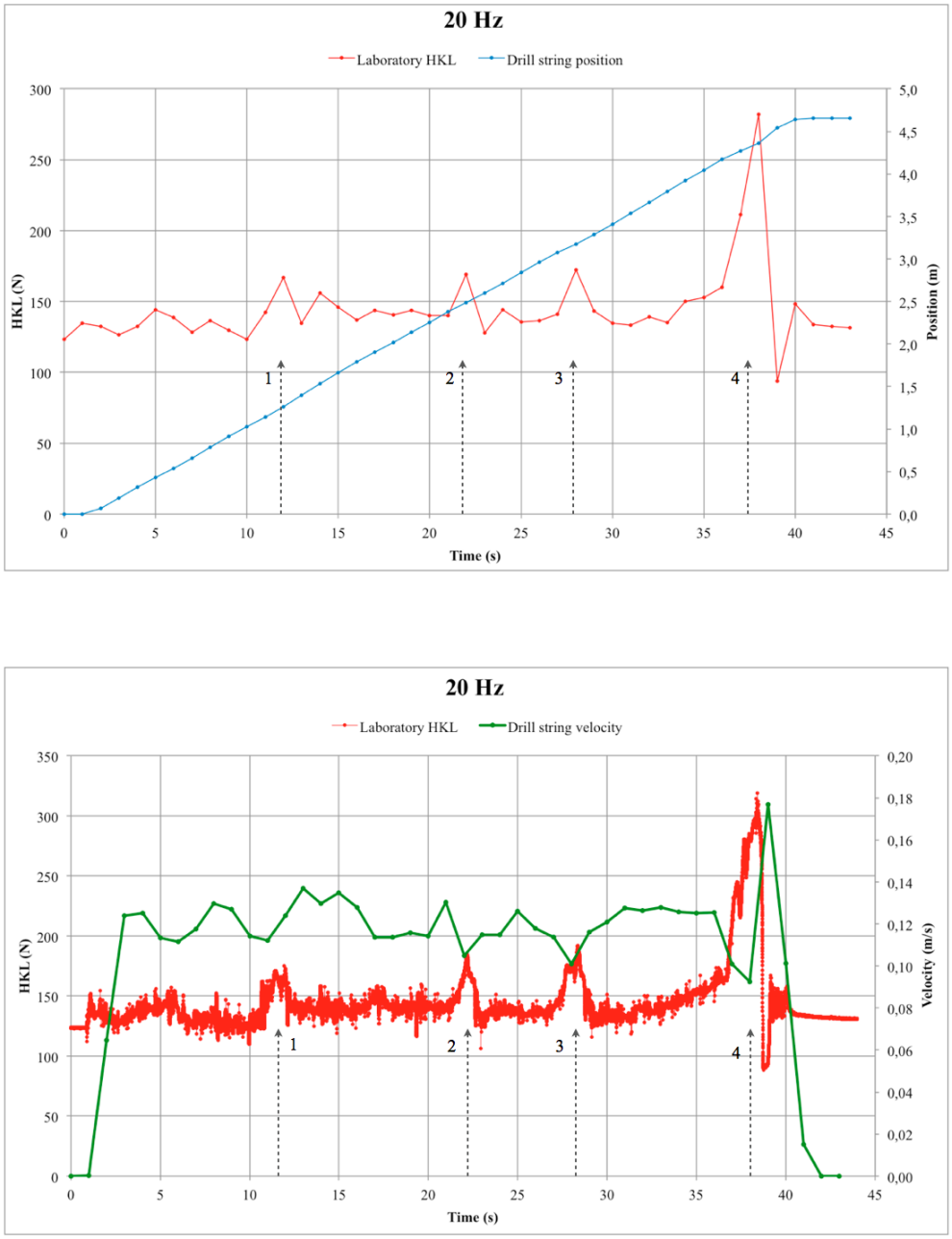

Figure 18: Test 1. No circulation or washout, low pulling velocity. Hook load and position, one measurement per second (upper view). Thousand hook load measurements per second (lower view). The arrows mark the peaks. Note how the velocity corresponds to the hook load value.

But the block velocity is assumed constant, and only the drill string acceleration is accessible in these results. Therefore, it is the drill string velocity that is presented together with the hook load results. From figure 18 (lower plot) it is observed that when the hook load increases the velocity of the drill string decreases, and when the hook load decreases the velocity increases.

There are four interesting incidents that should be studied more closely. They are marked in all figures with arrows numbered 1 to 4. These are peaks that are too high to be steady state peaks. In every test these peaks appear at approximately the same positions. These positions are found from the position graph in figure 18 and presented in table 6.

Table 6: Peak positions. Values are found from the position parameter in figure 18 (upper).

Peak 1	*Peak 2*	*Peak 3*	*Peak 4*
1,03 m	2,38 m	3,07 m	4,17 m

The first three peaks have just about the same behavior and value, while the fourth peak is much higher than the others. In this peak, the elasticity effect can be seen. After the high peak, the hook load value decreases to a low (negative) peak before returning to normal value. It is the string that stretches until the hook load force is large enough to overcome whatever restriction the drill string is experiencing, and the string contracts to its normal length again. Note how the velocity decreases correspondingly to the hook load peaks.

Clearly the plots with the higher sampling rate for hook load are most accurate. By comparing the hook loads in figure 18, it is seen that the lower hook load plot captures the average value better and thus highlights the peak behavior even better. With only one measurement per second the most extreme behavior may not be captured, or on the other hand, the spikes that occur may be captured, creating false peaks. The upper plot in figure 18 illustrates this weakness. In this plot it seems that there is a peak right after peak one, but in the lower plot the same hook measurements shows nothing but average hook load value. By comparing the upper and lower plot it is seen that the incorrect hook load behavior in the upper plot corresponds very well to the velocity in the lower plot. Nevertheless, these two hook loads correspond well.

Figure 19 presents the same as figure 18, only with medium instead of low

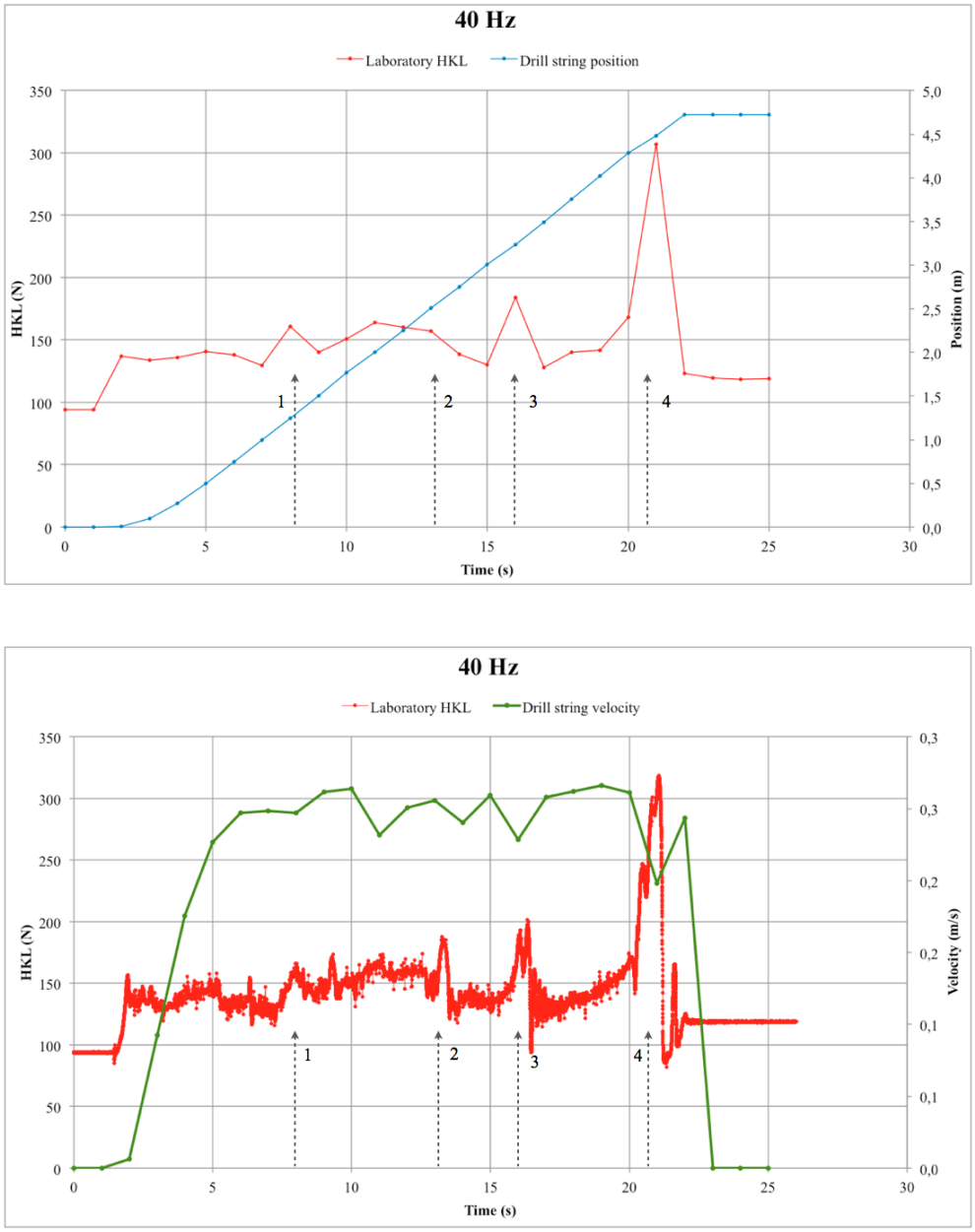

Figure 19: Test 2. No circulation or washout, medium pulling velocity. Hook load and position, one measurement per second (upper view). Thousand hook load measurements per second (lower view). The upper hook load does not quite manage to express peak number two or the low peak after peak four. Note how the drill string velocity corresponds to the lower hook load value. Note also the oscillating behavior after peak number two and three, and how the velocity does not correspond to the hook load during the second high peak.

pulling velocity. The conditions are identical. The same four peaks can be recognized, but there is something different. The hook load is oscillating more after the high peaks (see figure 19).

Due to the higher velocity but equal distance, fewer points are measured. Therefore the most accurate measurements are where the pulling velocity is low. For example, the upper hook load plot in figure 19 does not manage to express peak number two or the low peak after peak four. By looking at the drill string velocity at the time where peak two appears in the lower plot in figure 19, it is seen that the drill string velocity is not decreasing correspondingly, as it did for the low pulling velocity.

Figure 20 shows the results for high pulling velocity measurements. Here it is difficult to separate the peaks from eachother, it rather seems like there is something abnormal going on in the complete time interval (6 seconds to 12 seconds). The drill string velocity in figure 20 does not correspond with the lower hook load plot except from the period where peak three and four appear. Here, the velocity decreases as it should. Note how the hook load is oscillating even more at the high pulling velocity test.

The three tests presented here seem to be in accordance with each other. They all give approximately the same values for average hook load and for the high peaks, and register the same restrictions. The restrictions that cause these peaks will be looked further into later in this chapter.

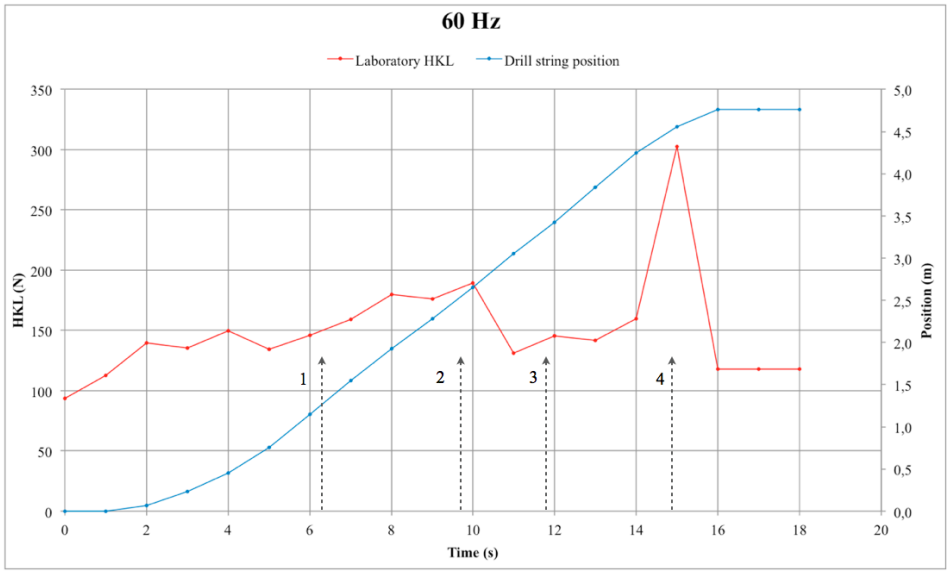

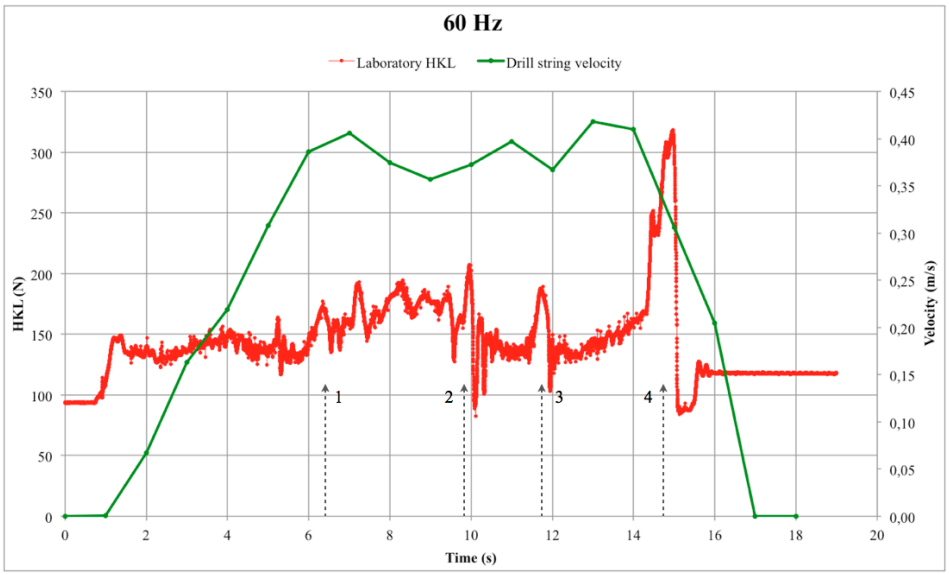

Figure 20: Test 3. No circulation or washout, high pulling velocity. Hook load and position, one measurement per second (upper view). Thousand hook load measurements per second (lower view). It seems that the higher the velocity, the more oscillation after peaks. Note that the upper hook load becomes less accurate as the velocity increase.

5.3.2 Testing with circulation

All laboratory experiments are of two types, one without circulation and one with circulation. The test matrix (table 4) gives a good overview. In this section the two results will be compared in order to see the effects of circulation. Fluidic drag must be taken into consideration; the friction may be affected. The drilling fluid functions as lubrication, which may lead to a lower mechanical friction. The flow rate is measured with a flowmeter, which is installed at the exit of the pump. The average flow rate was approximately 37 l/min for all tests.

In figure 21 the results from circulation with low pulling velocity are presented and compared with the result without circulation (test 1, figure 18).

The four peaks still occur, but their values have decreased. The average hook load value has decreased from approximately 140 N to about 125 - 130 N during circulation. The average hook load value is marked in the figures with a horizontal dashed line. The circles in figure 21 marks a time interval where results stand out compared to the results where there is no circulation. The hook load value is much lower than the average value, and it is constant. As the testing in the laboratory was conducted, it was observed that the drill string was moving faster than the block, making the wire slack. This low constant value is a result of higher drill string velocity than block velocity. The drill string position in the upper plot in figure 21 also indicates this. After this period of constant low hook load, the drill string is standing still, letting the wire tighten up, while the hook load value builds up again. This behavior is confirmed by the corresponding velocity measurements presented in the lower plot in figure 21. Pushing of the drill string caused the high drill string velocity peak, letting the wire slack. The tightening of the wire caused the low peak.

From this comparison it looks like the mud works as a lubricant, lowering the friction force. The drill string slides better during circulation. This is confirmed by the decreased high hook load peak values. But the phenomenon with the higher drill string velocity may be part of the explanation also. It seems like the mud flow pushes the drill string rather than creating a fluidic drag that pulls the drill string back. To obtain a better understanding of this, the higher velocity experiments must be analysed.

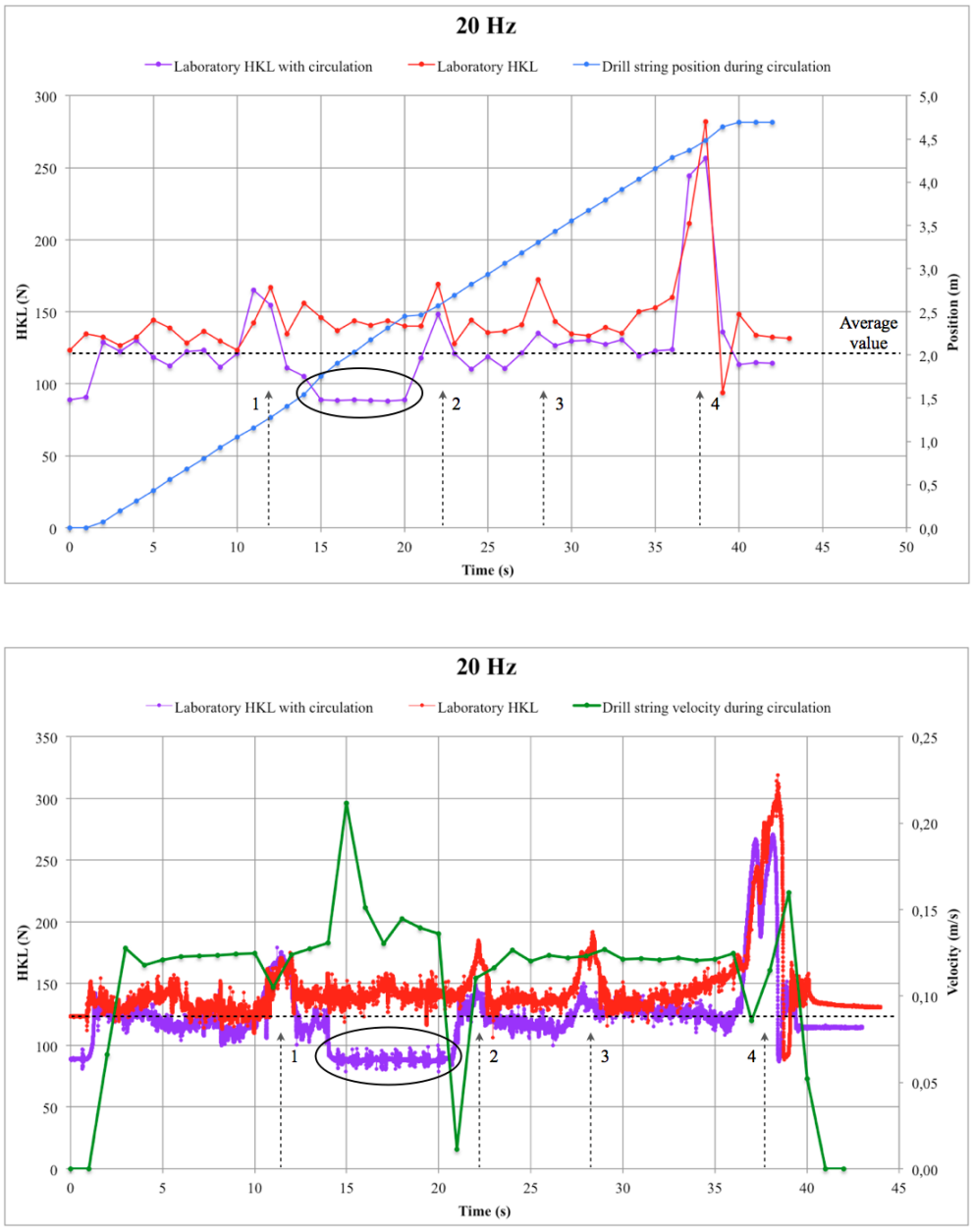

Figure 21: Test 4. Low pulling velocity, with circulation. Hook load and position, one measurement per second (upper view). Thousand hook load measurements per second, one drill string velocity measurement per second (lower view). The average hook load value marked with a dashed line has decreased compared to measurements without circulation. The circle marks the period where the mud velocity was higher than the block velocity. Note how the drill string velocity increase and decrease during this period.

Figure 22 presents the result with medium pulling velocity. The average value is a bit higher than for the low velocity test, and this low constant hook load marked with a circle is still pronounced. It is a bit more varying though, meaning that the drill string velocity is not constantly higher than the block velocity in the marked time interval. Note also how the average hook load value increases during tripping with circulation. This may be the effect of decreasing drill string volume in the annulus. The volume of the annulus increases as the drill string is pulled out. The mud velocity decreases, and the pushing force acting on the string decreases.

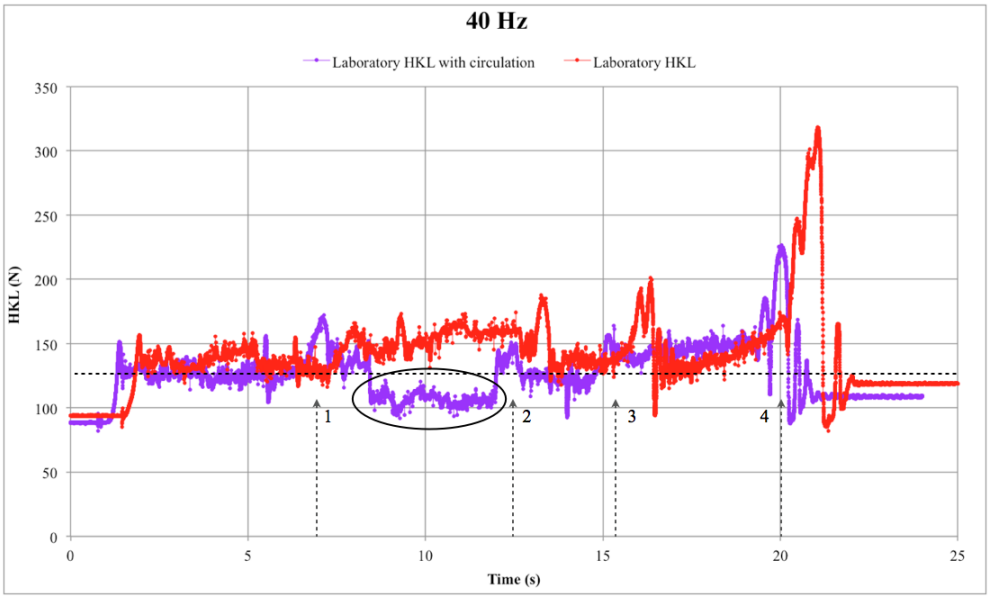

Figure 22: Test 5. Medium pulling velocity, with circulation. The dashed line marks the average hook load value. It has increased slightly again compared to the low pulling velocity measurement. Note how the hook load marked by the circle, varies more as the pulling velocity increase.

In the high pulling velocity test the constant low hook load value is no longer present. The circle marked in figure 23, which presents the high velocity test, shows no pronounced low hook load value. But the difference between the two results is distinguished, and shows a considerably lower average hook load value for the circulation test. Most likely the block velocity has increased past the mud velocity. The average hook load value is about the same as for medium velocity and the high peak values are still lower for the circulation test.

The lower the drill string velocity is, the higher the influence from the cir-

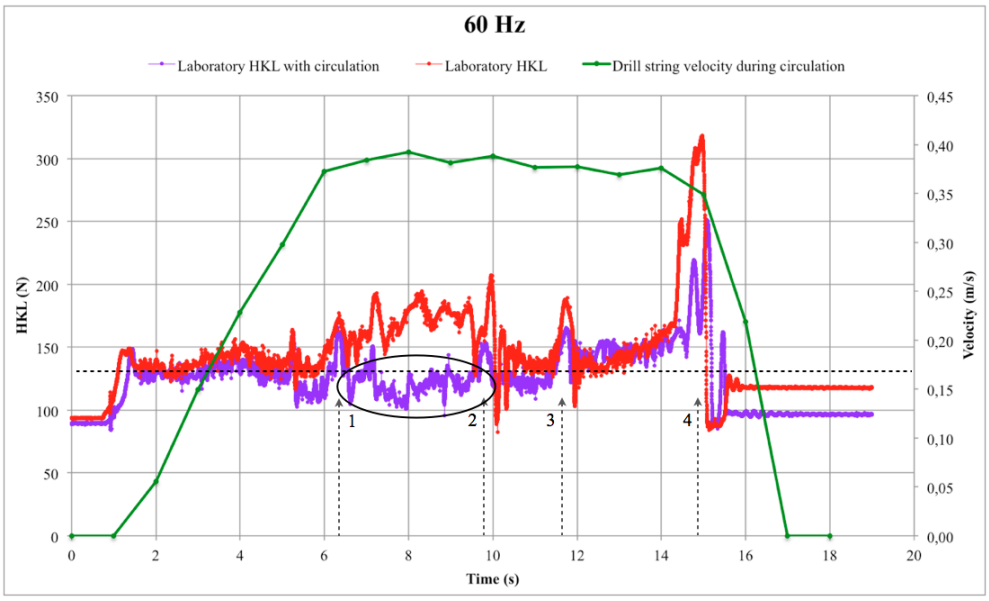

Figure 23: Test 6. High pulling velocity, with circulation. The hook load value marked by the circle is no longer much lower than the average hook load value. Most likely the block velocity has increased past the mud velocity.

culation is. If the mud velocity is higher than the block velocity the relative velocity will be negative, meaning that the fluidic drag works in the opposite direction (same direction as the drill string is being pulled). The low velocity is approximately 0,12 m/s according to measurements. In the annulus the mud velocity is the following:

$$v_{\text{mud}} = \frac{q_{\text{pump}}}{A_{\text{cs}}} \tag{38}$$

$$A_{\text{cs}} = \frac{\pi}{4}({ID_{\text{annulus}}}^2 - {OD_{\text{drill string}}}^2) \tag{39}$$

$$A_{\text{cs}} = \frac{\pi}{4}(0,0545^2 - 0,010^2) = 0,002254\ m^2 \tag{40}$$

$$v_{\text{mud}} = \frac{37\ l/min}{0,002254\ m^2} = 0,274\ m/s \tag{41}$$

The velocity of the mud is more than twice the velocity of the drill string, and it would be even higher along the BHA.

Since the average hook load value increases as the block velocity increase (decreasing the relative velocity between mud and drill string), it is reasonable to assume that part of the reason for the lower average hook load value is pushing of the drill string (as opposed to drag force).

5.3.3 Testing with expansion

For simulation of washouts, a part of the annulus has been replaced with a higher-diameter pipe. The inner diameter increased from 52 mm to 82 mm, an increase of about 50 %. There were used two different expansion pipes to simulate washouts. The first was slightly longer than the original exchangeable pipe (96 cm and 91 cm respectively) and the second expansion pipe was 20 cm. The test results from using the first expansion pipe are shown in figures 24 to 26 for the different pulling velocities respectively, together with the corresponding results where there was no washout.

Except from the oscillating effect, the results for the different pulling velocities are nearly identical. As in the previous tests, the four peaks marked in the figures are still distinct. There is some time delay between the two hook load results in the figures due to the manually starting of the simulations, but the peaks are really occurring at approximately the same time period. In figure 24 there is almost no difference in the results, the washout pipe does not seem to impact the friction or any other forces. But looking at figures 25 and 26 it is seen that something is changing.

It actually looks like the results without washout pipes installed (test 1-3) are the cause of the hook load difference. The average hook load value is stable for the washout results, but increases for the normal test results. Especially the period between peak one and two has a pronounced difference. From the position measurements the drill string position is 1,5 to 2,6 meters during this period. This corresponds to the period where the end of the BHA enters and exits the normal (slimmer) annulus (52 mm diameter instead of 82 mm).

The second expansion pipe has the same diameter as the first, but is about one fifth of its length (20 cm). The test result for low velocity is displayed in figure 27 together with the result without washout. Tests for medium and

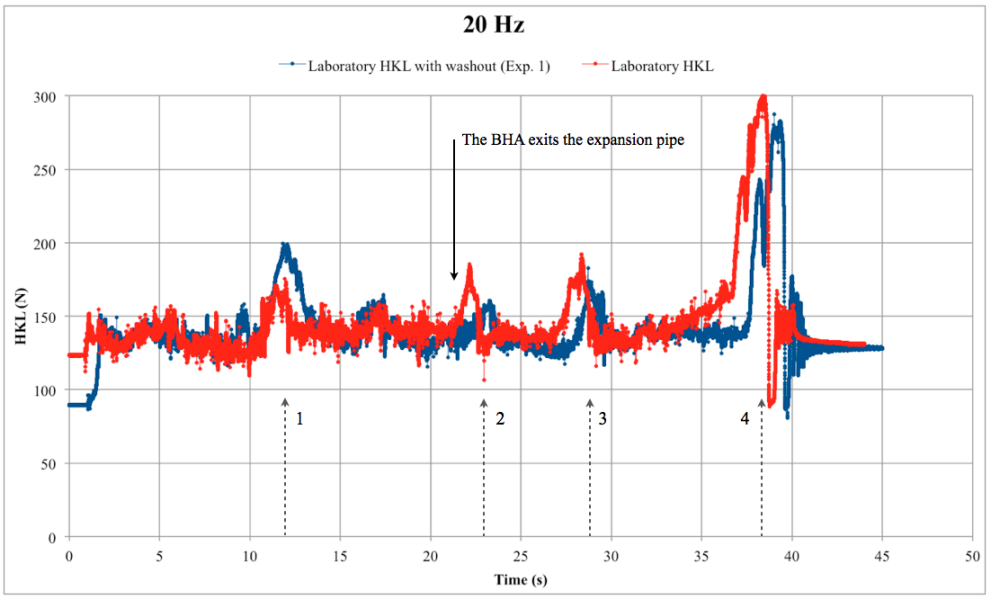

Figure 24: Test 7. Low pulling velocity, with washout (exp. 1). The difference between hook load with and without washout is small. No restrictions occur as the BHA exits the expansion pipe.

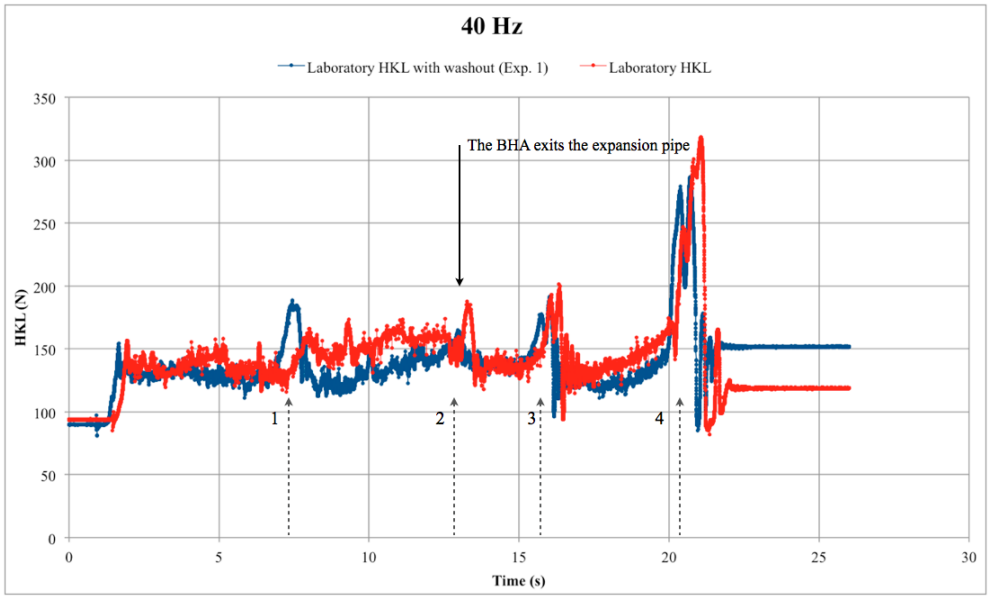

Figure 25: Test 8. Medium velocity, with washout (exp. 1). After the first peak, there is a distinct difference in average hook load value between the two tests. This period corresponds to the period where the end of the BHA enters and exits the slimmer annulus.

high velocity were executed, but the results were approximately the same as the low velocity results. As seen from the figure, the washout did not influence the results significantly.

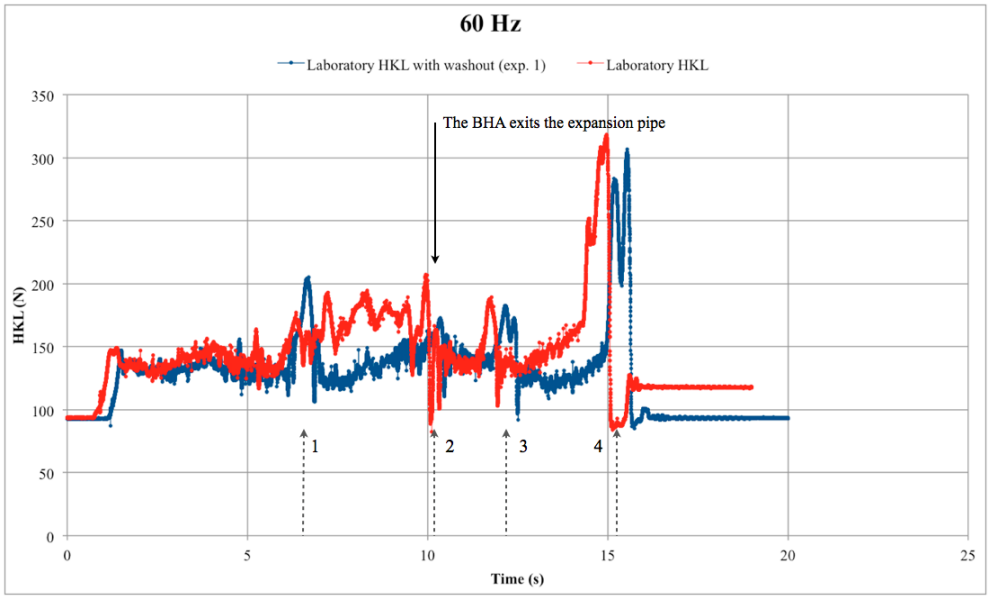

Figure 26: Test 9. High pulling velocity, with washout (exp. 1). The higher the velocity the more distinct the average hook load difference between peak one and two seems to be.

Tests with washout were also tested with circulation. The result is presented in figure 28. The average hook load value and the high peak values decreased with circulation. In contrast to the results for circulation without washout, there was no pronounced period with low constant hook load. With expansion pipes installed the annulus volume increases, leading to lower mud velocity. This could be the reason why this incident did not occur here.

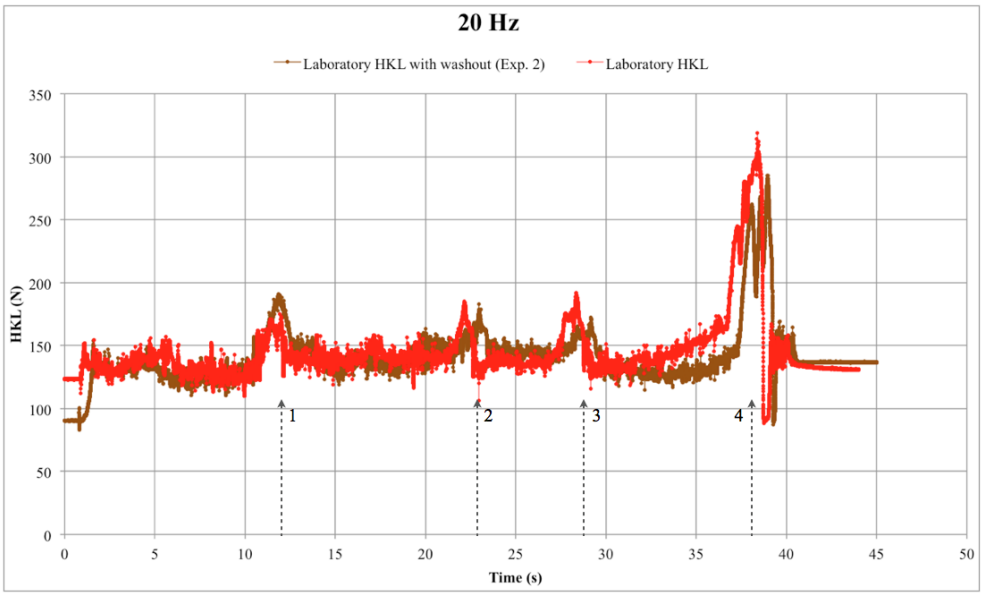

Figure 27: Test 13. Low pulling velocity, with short washout (exp. 2). The short washout pipe does not seem to have any impact on the hook load value.

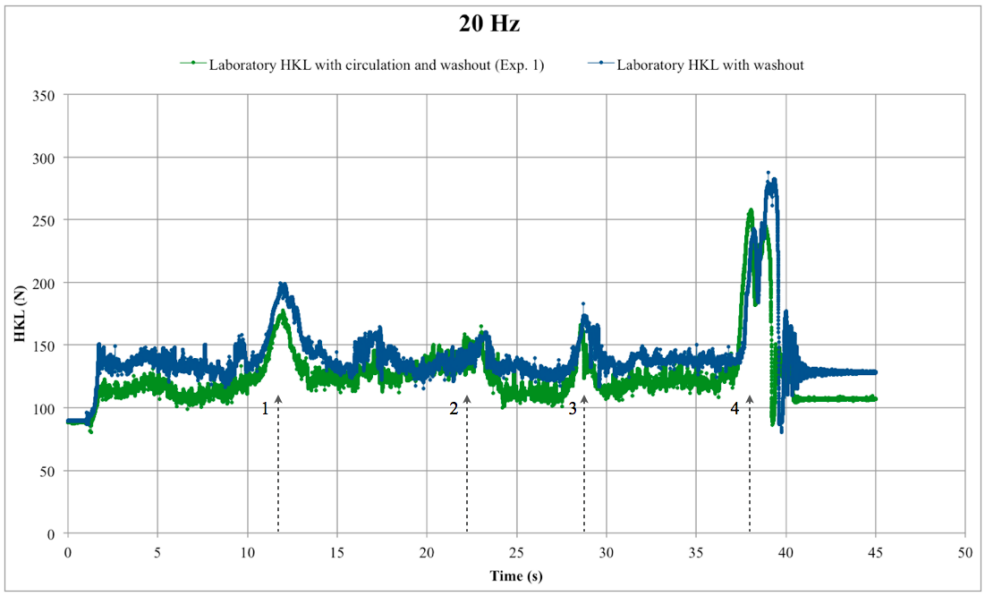

Figure 28: Test 10. Low pulling velocity, with washout (exp. 1) and circulation. Average hook load value and high peak values decrease as for other circulation experiments. The phenomenon with pushing of the drill string does not occur though.

5.3.4 Laboratory restrictions

Determining what is causing the peaks from the laboratory is important in order to make a good simulation model. It is necessary to determine how much circulation, washout, and other possible restrictions are affecting the hook load, and the relation between these parameters. It has already been stated that the friction is difficult to determine, and that the friction is used to explain the change in hook load if there are no other obvious reason.

It has also been stated that the pulling velocity corresponds to the high peaks. The question now is, what caused the pulling velocity difference for the drill string. Since the peaks arise in all tests, it does not come from washout or fluidic drag during circulation. The fact that the peaks arise in all experiments, the restrictions could be some sort of ledges. Ledges occur in the hook load measurements as an increase in hook load over a short time interval at the same position for every tripping that are made. By looking at the drill string element positions, there are no clear indications of any restriction in the annulus. The annulus is welded at some points, but no correspondence is found. The annulus exit is very tight; the opening matches the drill string diameter. The drill string itself is soft, and is therefore not completely straight, but slightly buckled. This will be discussed more thoroughly in the discussion chapter.

6 Comparing model with experimental results

Now that the results from the laboratory are analysed, a simulation model can be made based on the findings. The starting point of the models is equation 35 presented in chapter 4:

$$HKL(t) = F_{\text{weight}} + F_{\text{spring}}(t) + \sum_{n=1}^{N} F_{\text{f}}(t,n) + F_{\text{D,BHA}}(t)$$

The challenge is to calculate the F_{spring} and F_f correctly. F_{weight} is calculated based on input parameters and is constant. $F_{D,BHA}$ is calculated from the pump flow rate and the velocity is set for each test. The cross sectional area varies, but that is easily implemented. The friction force on the other hand, must be set based on real hook load values. A coefficient of friction must be set, simulations carried out, and then the resulting hook load and the real average hook load value must be compared. If the two average hook load values are similar, the right coefficient of friction is found, if not a new value must be set (see the flow chart, figure 6). The coefficient of friction will be programmed to fluctuate randomly around the set constant value to imitate the small steady state fluctuations.

The spring force is calculated based on the stretching of the string, and is the force that indicate the unforeseen restrictions. F_{spring} is the force that will simulate the high and low peaks. This should in theory not be too difficult, the spring constant is known and all the model needs is the stretch in the string at all time. The change in stretch is denoted dx, while length of the spring is denoted x.

$$dx(t) = v_{\text{block}}(t)dt - v_{\text{drill string}}(t)dt \tag{42}$$

$$x(t) = x(t-1) + dx(t) \tag{43}$$

The stretch of the spring is then equal $x(t)$ minus the initial length of the spring.

Due to the fact that block velocity is assumed constant and is calculated based on the average drill string velocity, and that the amount of measurements are low, the spring calculations becomes highly inaccurate. The spring is initially 20 cm long, and it cannot be compressed. The same correspondence as between drill string velocity and hook load, which was discussed and presented in figure 18, should be seen between the drill string velocity and dx (since dx changes proportionally to the drill string velocity). Figure 29 presents dx, velocity and stretch of the spring for test 1. Every time the velocity increase the dx decrease, and every time the velocity decrease the dx increase, the same way the velocity corresponds with the hook load. The stretch of the spring on the other hand behaves unrealistic. From about 15 seconds to 30 seconds the spring seems to be stretching from 0 cm to 8 cm. From observations in the laboratory, this is not correct. F_{spring} is proportional to the stretch of the spring, but in the simulations, adjustments are made to obtain a realistic F_{spring}. Basically the spring force will depend more on dx, rather than the unreliable stretch.

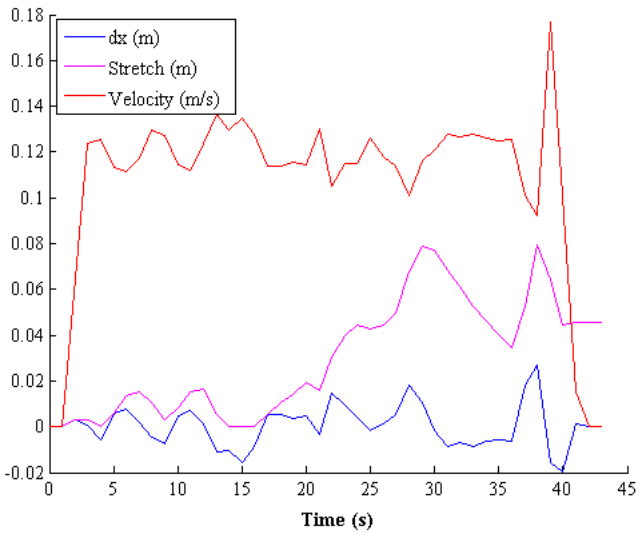

Figure 29: Drill string velocity with corresponding spring behavior. The same correspondence is found between dx and drill string velocity as between hook load and velocity in figure 18. As the velocity decrease the spring stretch (dx increase), and as the velocity increase the spring contracts again. The stretch of the spring presented in this graph corresponds poor with real drill string-as-a-spring behavior.

Simulations will only be carried out for the low velocity tests. The simulations are based on one measurement per second, and the 40 and 60 Hz

measurements have less than 25 measuring points in total. As the figures in chapter 5.3.1 stated, the hook load graph at high velocity becomes too inaccurate to base the simulations on.

6.1 Initial conditions

In the model the coefficient of friction is slightly increased during the period where the BHA travels through the normal (slimmer) annulus (see figures 24 to 26) to account for the increased average hook load value during this period.

Figure 30 presents the hook load measured in the laboratory together with the corresponding hook load simulated in Matlab. It is the low pulling velocity test with no circulation or washout. The simulated hook load follows the laboratory hook load in a satisfactory way. The average hook load value is similar, and the four high peaks are captured. It does look like the simulated peaks are a bit late compared to the laboratory hook load though, so another equation for calculating dx was tried (F_{spring} is proportional to dx).

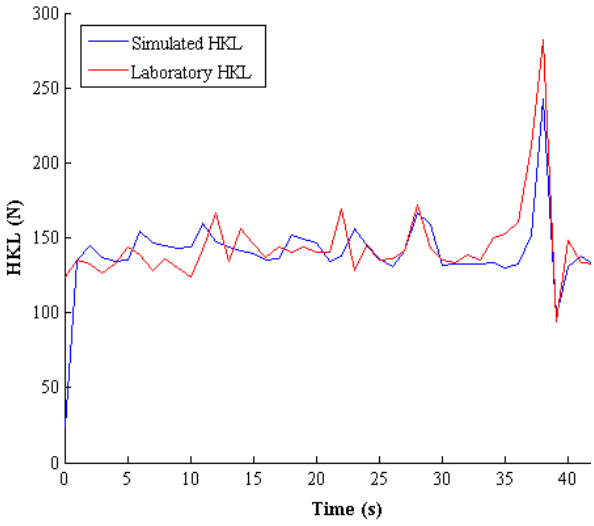

Figure 30: Hook load results from simulations and laboratory, test 1 (low pulling velocity). The two results are similar, but notice how the high peaks are a bit behind for the simulated hook load compared to the laboratory hook load.

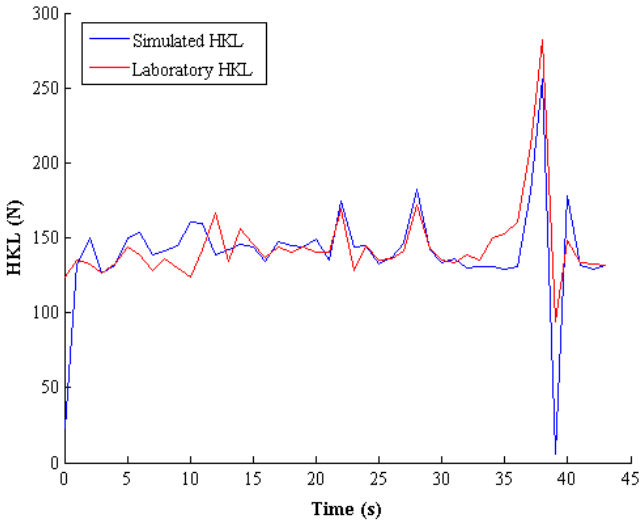

Figure 31: This is the same results as in figure 30, but with a different equation for dx calculations. Note the more edgy hook load graph for the simulated hook load and how the high peaks aren't behind anymore.

Equation 44 is the original equation, used in figure 30, while equation 45 is used in figure 31. The original equation uses the average velocity of two measurements, while the second equation uses the velocity measured at the current time. Changing equation for dx gives a more sharp-pointed, edgy hook load. The high peaks match very well with laboratory results. The low peak after peak four is, however, not a good match anymore.

Using the average of two measurements evens out the variations in the measurements, thus creating a dampening effect on the acceleration. Equation 45 does not have this effect, and therefore obtains some unrealistic hook load values when the acceleration has high positive or negative values. Further simulations will use a mix of these two equations. Equation 45 is used as default, but if the acceleration reach a certain value, equation 44 will be used to obtain dampening of the acceleration.

$$dx(t) = \frac{v_{\text{block}}(t) + v_{\text{block}}(t-1)}{2}dt - \frac{v_{\text{ds}}(t) + v_{\text{ds}}(t-1)}{2}dt \tag{44}$$

$$dx(t) = v_{\text{block}}(t)dt - v_{\text{ds}}(t)dt \tag{45}$$

The low velocity test with no circulation or washout was conducted several times. Another test result with the exact same conditions as the test presented in figure 30 is presented in figure 32. In this test, the hook load measurements have not captured any of the high peaks. The simulations were therefore not so good in this case. The two hook loads give the same average hook load value, and captures the low peak after peak four. but other than that they give high and low peaks at completely different time periods. The question is why the simulated hook load matches so well in figure 30, but so poor in figure 32.

To see if it was the equations in the model or the laboratory measurement itself that caused this poor hook load simulation, the measured drill string velocity and hook load were compared in figure 33 and 34. As previously mentioned, the peaks (restrictions) are indicated by the spring force, which again is calculated based on velocity measurements (see equation 44 for dx). In figure 33 and 34 measured hook load and velocity are presented for the tests in figure 30 and 32 respectively. In figure 33 the velocity and hook load seem to correspond as they should (see figure 18). When the hook load increases

the velocity decreases and vice versa. In figure 34 the same correspondence between hook load and velocity cannot be found, hence the poor simulation. Peak four is not simulated, because the laboratory measurements did not capture the decrease in velocity, the signature of the high peak.

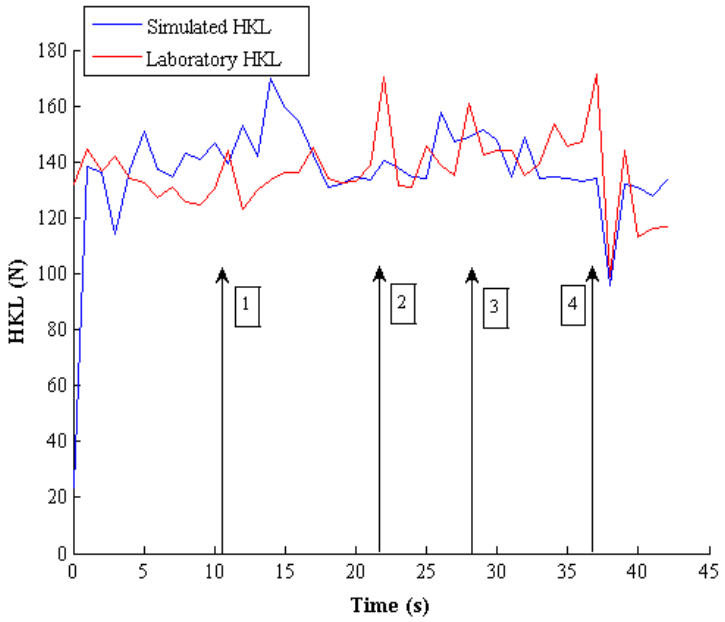

Figure 32: Hook load results from simulations and laboratory, test 1 (low pulling velocity). The simulation does not correspond very well with the laboratory result. Apart from the average hook load value and the low peak after peak four, high and low peaks occurs at different time periods for the two graphs.

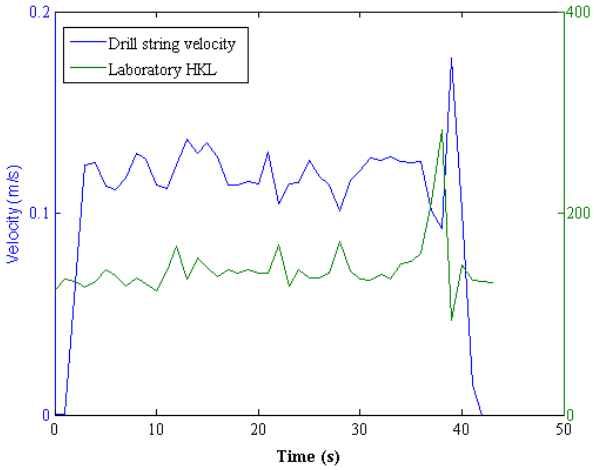

Figure 33: (Test 1, low pulling velocity) Comparison of the laboratory hook load and drill string velocity for the result with good simulation. See how the hook load and velocity corresponds. When the hook load increase the velocity decrease and vice versa.

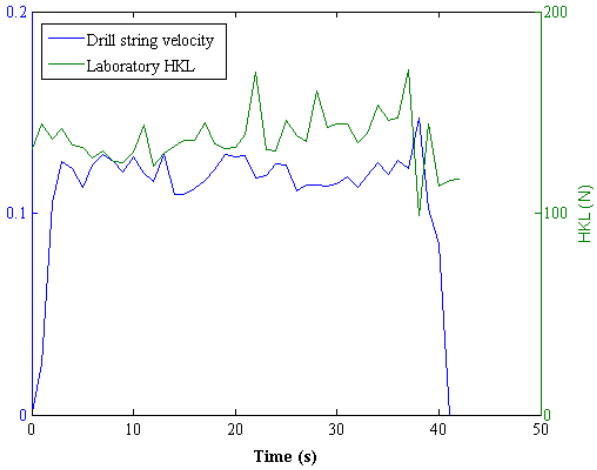

Figure 34: (Test 1, low pulling velocity) Comparison of the hook load and drill string velocity for the result with poor simulation. The correspondence found in figure 33 is not present for this test. Hence the poor hook load simulation.

6.2 Circulation simulations

The model also simulates hook load with flow in the annulus. In the model, the friction has been modified, and fluidic drag implemented. Figure 35 presents the laboratory and simulation hook load results. Looking at the two graphs, the model seems to manage circulation satisfying, as the hook load results are similar. But figure 36, which presents all contributing forces that adds up to the hook load, and the hook load itself, shows that the model does not behave optimal (the constant weight force is not included, since it is constant throughout the period).

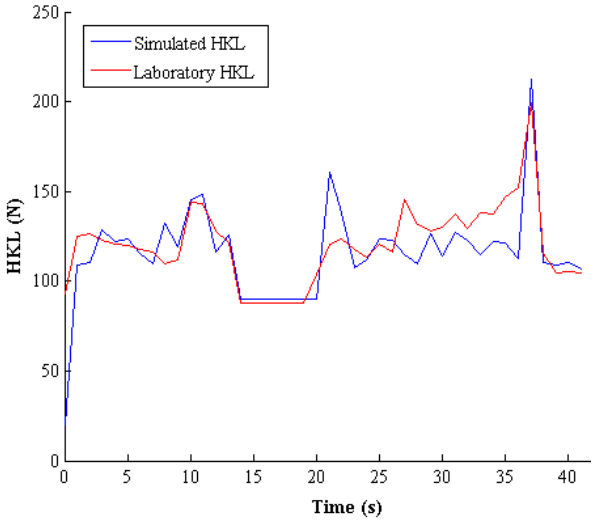

Figure 35: Test 4. Low pulling velocity, with circulation. Hook load results from the laboratory and simulations. The model seems to have captured the essential circulation behavior. But it has not manage to simulate the increasing average hook load value causes by decreasing mud velocity in the annulus.

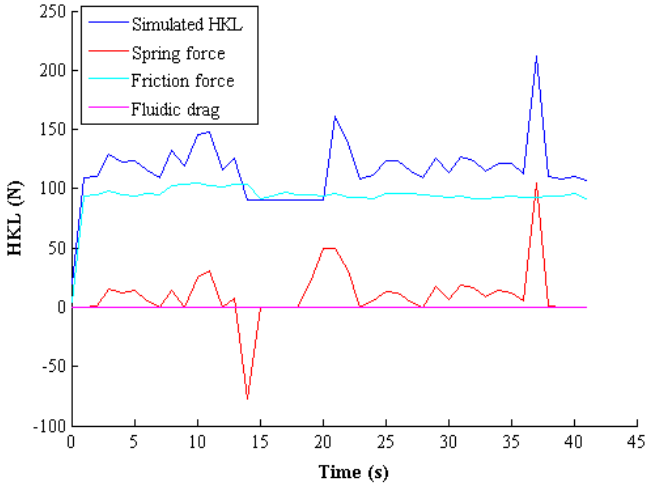

Figure 36: All simulated forces adding up to the hook load are presented (except the constant weight force). The fluidic drag is not modelled correctly, as it is close to zero the whole period. Instead the spring force has captured the phenomenon where the drill string is pushed, then almost stops while the wire tightens again.

The main 'problem' in the model is the mud flow behavior. From figure 36 it looks like the fluidic drag is constantly very close to zero. This is correct according to the mathematical equation presented for fluidic drag used in the model. Specifically, the fluidic drag fluctuates around -0,6 N (Negative due to the higher mud velocity). The fluidic drag is very small compared to the friction and spring force, which was predicted earlier. In reality it was experienced that the mud flow pushed on the drill string, causing the

wire to slack. This period is simulated with low hook load, as seen in figure 35. In the model the velocity behavior during this wire slacking has been used to recognize these phenomena, as it has been too difficult to describe mathematically. So it is not fluidic drag or other mud flow calculations that cause the low constant period, as it should be. The velocity behavior is expressed through the spring force. The low peak in the spring force indicates that the velocity increase rapidly. And the following high spring force peak indicate that the velocity decrease rapidly, which happens as the fluidic force no longer is high enough to push the drill string.

It was also mentioned that the average hook load value tends to increase as the drill string is pulled out of the annulus. This is also a consequence of the force from the mud flow (decrease as the drill string volume in the annulus decrease), and since the model has not been able to simulate fluidic drag or mud flow as it behaves in real, this phenomenon has not been simulated either. Hence the average hook load values differ towards the end in figure 35.

Figure 37 presents the results from another similar circulation test. As for the previous circulation test, the model does not manage to simulate the increase in average hook load value. In figure 38 the measured drill string velocity is presented together with the simulated hook load. The high increase in velocity correspond to the pushing of the drill string from the mud flow, and the following decrease indicate the period where the force from the flow no longer is strong enough to push the drill string. In this test, the phenomenon happened twice (the second immediately after the first).

By using the velocity measurements as an indicator of drill string pushing, the model is no longer mathematically correct. A trend in velocity measurements is used to correct the hook load and make it behave as it should. In both figure 35 and 37 this method shows weaknesses. In figure 35 the simulated hook load has an unnatural high value and increase after the drill string pushing phenomena. But the method can be quite spot on as well, as seen in figure 39. This is another similar test where the model simulation is very close to the laboratory hook load.

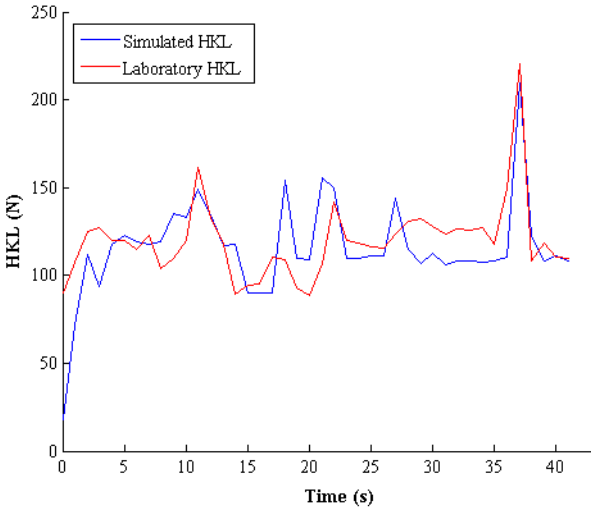

Figure 37: Test 4. Low pulling velocity, with circulation. Laboratory and simulation results from another circulation test. The comparison of these two hook loads shows that the model do not have optimal equations for the phenomenon with pushing of the drill string.

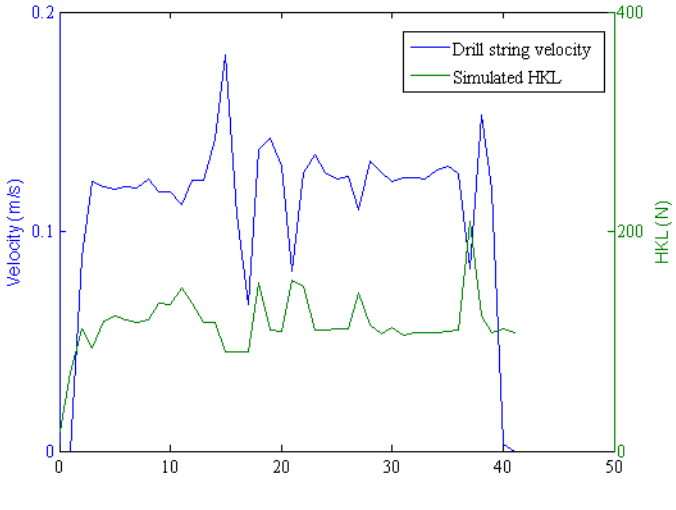

Figure 38: Test 4. Low pulling velocity, with circulation. Measured velocity compared with the resulting hook load simulation. Notice how the velocity increase as the hook load decrease and vice versa, and the characteristic behavior of the velocity when the drill string is pushed by the mud flow.

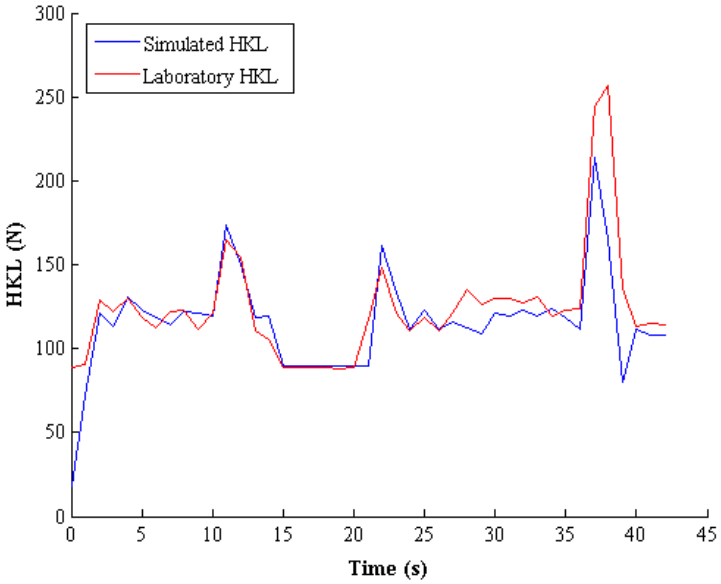

Figure 39: Test 4. Low pulling velocity. For this circulation test the model simulation matches the laboratory results in a satisfactory way.

6.3 Washout simulations

From the laboratory experiments the washout results did not give any characteristic behavior that differed from the other tests. They rather revealed the behavior of increasing friction for the normal (slimmer) annulus as the pulling velocity increased. In the model the change in cross sectional areas has been implemented. As the average hook load value did not change considerably for low velocity, the friction has not been changed for the washout zone.

Figure 40 presents the laboratory results together with the simulated hook load for washout (expansion 1). At the beginning of the test, where both the block and drill string are accelerated, the simulation displays a peak that are nowhere to be found in the laboratory hook load. Block acceleration is not measured, but estimated in the model. With few measuring points during the acceleration, the difference between drill string and block acceleration can be large for one measuring point, thus creating illogical behavior like this (see equation 44). In the time period from 10 seconds to 25 seconds the peaks are not coinciding with each other. Once again the velocity measurement is compared to the laboratory hook load to see if it is the velocity measurements that are poor. This comparison is presented in figure 41. The velocity does not quite correspond with the hook load measurements the whole period, and therefore some of the peaks appear at different times. But other than that, the simulation matches the laboratory results.

For simulations with both circulation and washout pipes installed, the results would be expected to be similar as for the circulation tests, but without the phenomenon where the hook load decrease due to higher mud velocity than drill string velocity (see figure 28). The simulation in figure 42 follows the same trend path as figure 40, but the simulations does not manage to simulate peak one or two. Figure 43 presents the drill string velocity corresponding to the hook load in figure 42 and it is seen that the velocity is more steady than the velocity in figure 41. Due to this low velocity variation, the variation in forces becomes low. But other than this, they behave similar and the average hook load value decreases as expected. Compared to experiments with circulation and no washout (see figure 39), it is seen that the phenomenon with the low hook load value does not appear, which also was expected.

Several tests have been conducted and simulated, but not presented. All the

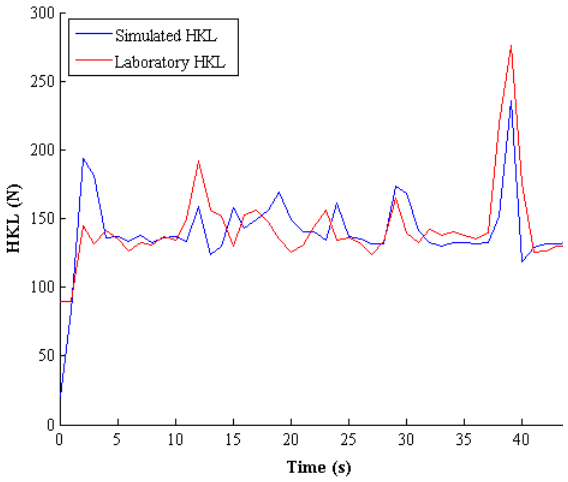

Figure 40: Test 7. Low pulling velocity, with washout (exp. 1). Apart from some peak appearance differences, the results mostly corresponds, and simulations are satisfying.

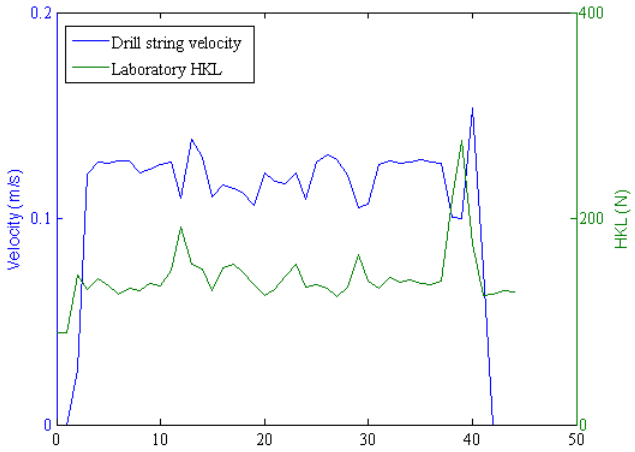

Figure 41: The velocity does not completely correspond with the hook load. Hence the difference between the laboratory peak measurements and simulated peaks.

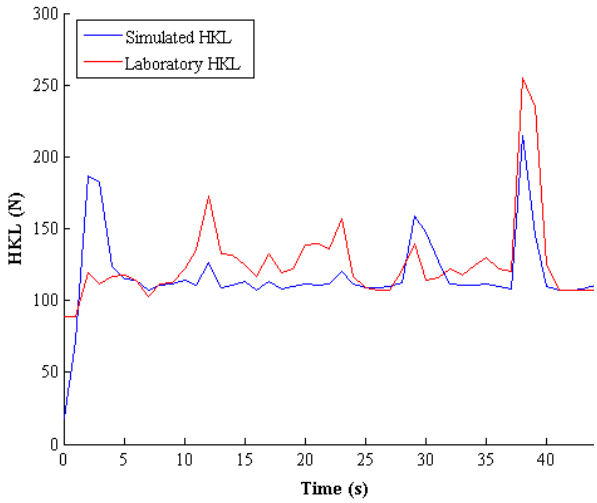

Figure 42: Test 10. Low pulling velocity, with circulation and washout. The average hook load value is good, but only two of the four peaks are captured.

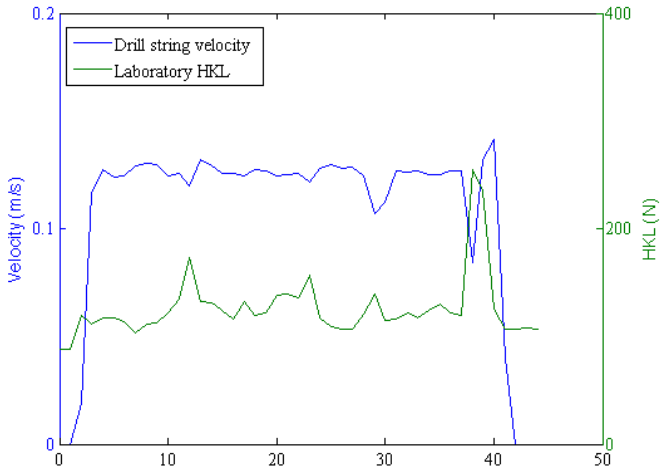

Figure 43: The velocity corresponds to the hook load, but varies little compared to other experiments (see figure 41). Hence the poor peak simulations in figure 42.

essential behavior has been presented through the figures in present report.

7 Discussion and evaluation

A model has been created and presented in chapter four, based on a paper from Mme et al., (2012). The simulation results of the model were acceptable, but have room for improvements. The main goal was to simulate the hook load under the simplest conditions during tripping, which is without drilling fluid circulation and wellbore washout. From the results it can be concluded that this goal was achieved. But for fluid circulation conditions the model turned out to be weak because it did not manage to mathematically describe all events during circulation.

7.1 Quality of input data

The model simulates hook load based on position measurements from laboratory experiments and on equipment specifications from the laboratory set up. This includes parameters like length of different pipes and equipment, diameters, mass and density of pipes and fluids. Uncertainties and possible errors occurs since some input data are measured manually and the laboratory set up is not optimized.

The laboratory was build with equipment and tools that are not in proportion with each other. It was stated previously in the report that the reason why 'first high peak' (Coulomb friction) did not occur in the experiments was low mass of the drill string. The first high peak is a consequence of the inertia force (the resistance of any physical object to change its state of motion or rest). Due to the high mass of a real drill string it takes a higher force to start its motion than keeping it in motion. The higher mass, the higher force is needed to accelerate it. Another example of bad proportions was the diameters of the BHA and drill pipe; the BHA diameter was five times the diameter of the drill string. The clearance in the annulus and the velocity of the mud and drill pipe are other examples worth mentioning. The result of inadequate proportions are that incidents that does not occur in the field occur in the laboratory, making it difficult to create a general model that will apply for both the laboratory and field input data.

The block acceleration is critical for interpreting the hook load since the hook load is measured from the dead line tension in the field. In the laboratory

the hook load depends on both block and drill string acceleration due to the installed spring. It is assumed that the block velocity in the laboratory is constant except for at the beginning and end of the test where it accelerates. In the laboratory measurements, only the drill string acceleration can be found. The block acceleration is not measured, but implemented in the model based on observations in the laboratory. In the model, this implementation is one of the most important causes for errors in the simulation.

The most important input data is the position and hook load measurements from the experiments. The laboratory setup was not used before experiments were executed for this thesis. Thorough procedures for running them were not created in advance. The laboratory is constructed in a way that requires manually starting and stopping of the motor. The starting position of the drill string is set manually and the initial slack of the wire was difficult to adjust equally for every test. Thus, the acceleration pattern for initiating the pulling and length of the tripping also varied, creating variations in relative position for each experiment and making it difficult to mathematically describe the block velocity at the start.

When it comes to the measurements themselves the rate of position measurements is too low. The rate of hook load measurements is a thousand measurements per second, which makes the hook load reliable. But the drill string position is read in Labview once per second, making it difficult to register all incidents during an experiment. This issue has been thoroughly presented in the results. The drill string velocity and acceleration, which are calculated from the position measurements and are the foundation for hook load calculations in the model, becomes inaccurate.

7.2 Quality of the model

The results showed that the model managed to simulate the hook load close to the real laboratory value. The average hook load value, which is determined by the weight and friction force, was mostly accurate. The random fluctuation around the set coefficient of friction worked successfully. During simple conditions, which was without formation washout or fluid circulation, this model worked satisfactory. The equation for calculating the changes in hook load from average value responded well to the measured velocity. The errors for the simulated peaks are mainly believed to be a cause of the inac-

curacy in the velocity calculations from the measurements. The calculated behavior of dx and corresponding extension of the spring confirms this. But it could also be that the equation for calculating the spring force should be improved, this can only be checked by obtaining better measurements.

The model is limited to measurements conducted with low velocity (20 Hz). There are two main reasons for this; the first is that there are so few measurements during high velocity experiments that further calculations on the position measurements become too inaccurate. The second reason is that there is no accurate mathematically formula for calculating the block acceleration at the beginning and end of an experiment (since it is based on observations), thus making the formulas implemented in the model wrong for pulling velocities other than 20 Hz. Of course, acceleration for 40 and 60 Hz could be implemented, but again this would lead to large errors in the calculations. It is unfortunate that only low velocity experiments are implemented in the model since the results showed that velocity changes affected the hook load behavior.

It turned out that increasing velocity gave more oscillating effects when restrictions (peaks) occurred, and increased hook load as the BHA travelled through the slimmer part of the annulus. Why this is the case is difficult to say, because the velocity does not affect the friction force according to the equation for friction.

During circulation the model gave the least accurate hook load simulation. As circulation is started, the coefficient of friction decrease, resulting in a lower average hook load value and peak value in accordance with the laboratory hook load during circulation. The major weakness of the model is the mud flow force calculations. As presented in the results there were periods where the mud flow pushed the drill string rather than creating a fluid drag that works in the opposite way. In the field, situations like this do not occur. Most likely it is the wrong proportions of the laboratory that causes this phenomenon. The mud velocity is more than twice the drill string velocity, which is not normal in the field.

The model for fluidic drag does give a negative force during this phenomenon, thus decreasing the hook load as it should. But the value of the fluidic drag in the model is too low compared to the observations in the laboratory. This has most likely led to a larger decrease in the coefficient of friction in the model than what really is the case. The simulation also reflects this, because as the

drill string is pulled out of the annulus, the difference between simulated and laboratory average hook load value increase. What happens in the laboratory experiment is that the drag force from the mud flow decrease (mud velocity decrease due to decreasing drill string volume in the annulus), thus increasing the average hook load value. In the simulations on the other hand, the fluidic drag and friction force remains constant.

Assumptions were made regarding the fluidic drag in the model. It was said that the mud velocity was the same along the cross section of the annulus. In reality the mud velocity is zero at the pipe walls and maximum in the middle of the flow profile. This assumption might be a cause for the poor fluidic drag simulations, but also other parameters could be wrong; the viscosity of the water is not measured, and the water is not entirely clean. It is not 20 °C in the laboratory room either. Only the drag force from the fluid acting on the BHA is taken into consideration. Any force from the fluid acting on the BHA end cross sectional area is not accounted for, and this is probably a part of the error.

7.3 Future improvements

The foundation for achieving good and accurate measurements is a laboratory setup that leaves little room for measuring errors and that does not allow the user to create uncertainties in the measurements. A proper list of equipment measures and a more automated laboratory should therefore be created if further experiments were to be executed. After tripping out the drill string, one must push the drill string back into the annulus themselves. If the drill string is pushed entirely back into the annulus, the end piece of the drill string, which has larger diameter, interfere with the position measurer and must therefore be pulled back out a few centimetres. Manually stopping the drill string makes it difficult to stop at exactly the same position in every experiment. Starting and stopping of the experiment, and simultaneously start and stop the Labview program should therefore be an automated process.

The Labview program should in the future record position measurements with the same rate as the hook load measurements. It is possible to observe the position change continuously on the screen, so it should also be possible to program the Labview program to increase the rate of measurements.

In addition, the laboratory should implement block position measurements. Having both drill string and block acceleration would make the model more accurate. Calculation of the spring force would be better, thus making the peak simulations more accurate. By increasing the measurement rate, the steady state fluctuations would improve as well.

If the model were to be used for tripping with circulation, the calculations for fluidic drag and other mud flow forces would need a lot of improvement. With the laboratory as it is, the phenomenon of pushing the drill string must be explored. To understand why the mud flow forces are so high in inclined wells, where several sources for this thesis has concluded that the friction force is the dominating force is important. For example, the possible force from the fluid acting on the exposed BHA and cross sectional area must be included.

The model is adjusted to the input data from the laboratory at this point. This was done partly because a vital parameter is missing (the block position), but also because there was little time to try making the model more general than it is now. The input data from the laboratory (equipment measurements) should be easier to change. Maybe it should be required that data like length and diameter of drill pipe and BHA must be typed in before running the simulation. This would make the model more general, thus making it easier to run RTDD with it. And when it is possible to run RTDD in the model, comparison of simulations and field results would be possible.

It is difficult to say whether the model is realistic to be run with real field data, as the model has not run any RTDD. It could be difficult also since the model builds on drill string position instead of block position. But the principle is the same, so it should not be too difficult to switch between these parameters. Ideally, the laboratory would measure the block position, and this parameter would replace the drill string position. Real drill strings some times experience compressing during tripping, but the spring in the laboratory cannot be compressed. Installing a spring that is able to compress could improve the spring stretch calculations, and thus contribute to a more realistic model. Also, installing a softer spring (a spring with low spring constant) might result in a 'First high peak' in the laboratory results.

The reason why the four peaks that has dominated the laboratory results in every experiment occur should be stated. It has been suggested that it is some sort of ledges or shoulders that cause them, and the period where the

peaks arise has been investigated, but no clear restrictions has been found. The last proposal was that the exit of the annulus is causing these peaks. If further experiments were to be executed, the exit should be examined.

8 Conclusion

- A hook load model based on laboratory experiments has been successfully made. Under simple conditions the model creates good and accurate hook load simulations.
- For further experiments the laboratory set up should be more automated, and a detailed running procedure worked out. Then, the input data will be more reliable.
- The rate of drill string position measurements read into the Labview program must be increased and block position measurements implemented in order to obtain a more mathematically correct model.
- The flow behavior must be investigated, and the fluidic drag equation improved. The simple fluidic drag equations in the model led to poor match during tripping simulations.
- It is difficult to say it the existing model is realistic, as RTDD has not been run in the model. To enable running of RTDD into the model, the model needs to become more general, and block velocity must be able to vary. This can be solved with better measurements and thus more general mathematical equations.

Nomenclature

Abbreviations

BHA Bottom hole assembly

BPOS Block position

COF Coefficient of friction

HKL Hook load

ID Inner diameter

NPT Non-productive time

OD Outer diameter

RTDD Real time drilling data

Parameters

A_{cs} cross sectional area

B buoyancy force

F_{axial} axial force

F_{D} fluidic drag force

F_{dl} deadline tension

F_{f} friction force

F_{n} normal force

F_{spring} Spring force

F_{weight} weight force

G gravity force

G_{y} gravity component in the y-direction

L length of element

β buoyancy factor

λ	elastic modulus
μ	coefficient of friction
μ_{k}	kinetic coefficient of friction
μ_{mud}	mud viscosity
μ_{s}	static coefficient of friction
ϕ	azimuth
ρ_{fluid}	fluid density
ρ_{mud}	mud density
ρ_{steel}	steel density
σ	material stress
τ	shear stress at pipe surface
θ	inclination angle
ε	material strain
a	acceleration
d_{h}	diameter of annulus
d_{s}	diameter of the string
g	gravity constant
k	spring constant
m	mass of element
q_{pump}	pump flow rate
v	relative velocity
v_{block}	block velocity
v_{ds}	drill string velocity
v_{mud}	cross sectional mud velocity
w	weight of component

w weight of drill string element

Symbols

Hz Hertz

N Newton

cm centimeters

m meters

mm milimeters

References

Schlumberger (2012). *'Hook load'*. http://www.glossary.oilfield.slb.com/Display.cfm?Term=hook%20load

Mme, U., Skalle, P., Johansen, S. T. and Sangesland, S. (2012). *'Analysis and modeling of normal hook load response during tripping operations'*. Not yet published.

Luke, G. R. and Juvkam-Wold, H. C. (1992). *'Determination of True Hook Load and Line Tension Under Dynamic Conditions'*. Paper 23859, SPE. Presented at the1992 IADC/SPE Drilling Conference, New Orleans, Feb 18-21.

'Gravitation'. Wikipedia (2012a). http://en.wikipedia.org/wiki/Gravitation

'Buoyancy'. Wikipedia (2012b). http://en.wikipedia.org/wiki/Buoyancy

'Friction'. Wikipedia (2012c). http://en.wikipedia.org/wiki/Friction

Belaskie, J. P., McCann, D. P. and Leshikar, J. F. (1994). *'A Practical Method To Minimize Stuck Pipe Integrating Surface and MWD Measurements'*. Paper 27494, IADC/SPE. Presented at the 1994 IADC/SPE Drilling Conference, Dallas, Feb 15-18.

Bible, M. J., Hedayati, Z. and Choo, D. K. (1991). *'State-of-the-Art Trip Monitor'*. Paper 21965, SPE/IADC. Presented at the 1991 SPE/IADC Drilling Conference, Amsterdam, March 11-14.

Mirhaj, S. A., Fazaelizadeh, M., Kaarstad, E. and Aadnoy, B. S. (2010). *'New Aspects of Torque-and-Drag Modeling in Extended-Reach Wells'*. Paper 135719, SPE. Presented at the 2010 SPE Annual Technical Conference and Exhibition, Florence, September 19-22.

Polak, M. A. and Lasheen, A. (2002). *'Mechanical modelling for pipes in horizontal directional drilling'*. Paper, Pergamon. Tunnelling and Underground Space Technology 16 Suppl. 1, S47-S55. http://www.sciencedirect.com/science/article/pii/S0886779802000202

Maidla, E. E. and Wojtanowicz, A. K. (1987). *'Field Comparison of 2-D and 3-D Methods for the Borehole Friction Evaluation in Directional Wells'*. Paper 16663, SPE. Presented at the 62nd SPE Annual Technical Conference and Exhibition, Dallas, September 27- 30.

Skalle, P. (2010) *'Drilling Fluid Engineering'*. Ventus Publishing ApS. http://bookboon.com/en/textbooks/geoscience/drilling-fluid-engineering

Aadnoy, B. S., Cooper, I., Miska, S., Mitchell, R. F. and Payne, M. L. (2009). *'Advanced Drilling and Well Technology'*. Vol. 1, published by SPE.

Oilfield Glossary (2012). *'Keyseat'*. http://www.glossary.oilfield.slb.com/Display.cfm?Term=keyseat

Massareli, P. (2012). *'Introduction to engineering, section 19 & 20'*. http://people.virginia.edu/ pjm8f/engr162/beam/stress_and_strain.htm

Appendices

A The model Matlab code

Since the position was measured only every thousand time the hook load was measured, a function was created in order to extract the hook load data that corresponds to the position measurements. This function is displayed here:

```
function[time,position,hook,velocity,acceleration] = extract_rev3

% reads the excel file created by Labview:
Matrix = xlsread('20HzCircExt1');

TIME = Matrix(:,1);
Hookload = Matrix(:,2);
Pulse = Matrix(:,3);
count = 0;

Hookload = -50.*Hookload;  % converts HKL force to Newton.
Pulse = Pulse./5000;       % converts position into meters.

time(1,1) = 0;
position(1,1) = 0;
hook(1,1) = 0;

for i = 1:1000:length(Pulse)
    count = count + 1;
    position(count,1) = Pulse(i); % extract every measurement
    time(count,1) = TIME(i);      % extract every thousand measurement
    hook(count,1) = Hookload(i);  % extract every thousand measurement
end

dt = diff(time);
velocity(1:length(position),1) = 0;

for n = 2:1:length(time)
```

```
    velocity(n,1) = (position(n) - position(n-1))/dt(n-1);
end

acceleration(1:length(position),1) = 0;

for m = 2:1:length(time)
    acceleration(m,1) = (velocity(m,1) - velocity(m-1,1))/dt(m-1);
end
end
```

The main Matlab script calculated the different forces acting on the string and summed them together.

```
Circ = 0; % no circulation
%Circ = 1;  % circulation
c = 0;
posMax = 0;
posMin = 0;

Length_ds = 4.9; % metres
Length_BHA = 0.93;
Length_Ann = Length_ds + Length_BHA;

OD_ds = 0.01; % metres
OD_BHA = 0.049;
ID_Ann = 0.0545;
OD_Ann = 0.060;
N = 10;       % number of elements

Inclination = 84*pi()/180; % degrees to radians
Steel = 7850; % kg/m3
Mudweight = 1000; % kg/m3
g = 9.81;         % gravity constant
visc_mud = 0.001; % Pa*s, for water

ext0=[0.91 4.12 3.21]; % length start stop, metres from annulus exit
ext1=[0.96 4.17 3.21];
```

```
ext2=[0.2 3.47 3.27];

ID_ext0 = 0.052;  % metres
ID_ext1 = 0.082;
ID_ext2 = 0.082;

% cross sections areas in the annulus

a_ann_BHA = pi()/4*(ID_Ann^2 - OD_BHA^2);
a_ann_ds = pi()/4*(ID_Ann^2 - OD_ds^2);
a_ext0_BHA = pi()/4*(ID_ext0^2 - OD_BHA^2);
a_ext0_ds = pi()/4*(ID_ext0^2 - OD_ds^2);
a_ext1_BHA = pi()/4*(ID_ext1^2 - OD_BHA^2);
a_ext1_ds = pi()/4*(ID_ext1^2 - OD_ds^2);
a_ext2_BHA = pi()/4*(ID_ext2^2 - OD_BHA^2);
a_ext2_ds = pi()/4*(ID_ext2^2 - OD_ds^2);

if Circ == 1
    bouyancy = 1 - (Mudweight/Steel);
else
    bouyancy = 1;
end

Mass_ds = pi()/4*(OD_ds^2)*Steel; %kg/m
Mass_BHA = pi()/4*(OD_BHA^2)*Steel; %kg/m

pump_rate = 0.00062; % m3/s
my_static = 0.4;     % experimentally set

Length_n = Length_ds/(N-1); % excluded the BHA
mass_n = Length_n*Mass_ds*bouyancy;      % kg
mass_N = Length_BHA*Mass_BHA*bouyancy;   % kg
k = 2730;                                % N/m

% using the function to extract correct data:

[TIME,BPOS,True_HKL,Velocity,Acceleration] = extract_rev3;
pull = diff(BPOS);  % distance travelled between every measurement
```

```
M = length(TIME);   % number of measurements

u(1:M,1:N) = 0;
A(1:M,1:N) = 0;     % cross section area for element n at time t
D(1:M,1,N) = 0;
u(1,N)=Length_Ann; % positions are metres from the start of annulus
for n = 1:1:N-1
    u(1,n) = n*Length_n;
end
for t = 2:1:M
   for n = 1:1:N
      u(t,n)=u(t-1,n)-pull(t-1); % position change for each element
   end
end

% CROSS SECTIONAL AREAS WITH EXPANSION INSTALLED:

%for n = 2:1:N-1  % cross section area for all drill string elements
%    for t = 1:1:M
%        if u(t,n-1) < 0
%            A(t,n) = 0;
%        elseif u(t,n-1) < ext1(2) && u(t,n-1) > ext1(3)
%            A(t,n) = a_ext1_ds;
%            D(t,n) = ID_ext1;
%        else
%            A(t,n) = a_ann_ds;
%            D(t,n) = ID_Ann;
%        end
%    end
%end

%for t = 1:1:M       % cross section area for BHA
%    if u(t,N-1) < ext1(2) && u(t,N-1) > ext1(3)
%        A(t,N) = a_ext1_BHA;
%        D(t,N) = ID_ext1;
%    else
%        A(t,N) = a_ann_BHA;
```

```
%        D(t,N) = ID_Ann;
%    end
%end

% CROSS SECTIONAL AREAS WITH NO EXPANSION INSTALLED:

for n = 2:1:N-1  % cross section area for all drill string elements
    for t = 1:1:M
        if u(t,n-1) < 0
            A(t,n) = 0;
        elseif u(t,n-1) < ext0(2) && u(t,n-1) > ext0(3)
            A(t,n) = a_ext0_ds;
            D(t,n) = ID_ext0;
        else
            A(t,n) = a_ann_ds;
            D(t,n) = ID_Ann;
        end
    end
end

for t = 1:1:M       % cross section area for BHA.
    if u(t,N-1) < ext0(2) && u(t,N-1) > ext0(3)
        A(t,N) = a_ext0_BHA;
        D(t,N) = ID_ext0;
    else
        A(t,N) = a_ann_BHA;
        D(t,N) = ID_Ann;
    end
end

Fdrag(1:M,1) = 0;
Ff(1:M,1:N) = 0;
sum_HKL(1:M,1) = 0;
my_kinetic(1:M,1:N) = 0;
R1 = rand(M,N);
R2 = rand(M,N);

for o = 1:1:M
```

```
  for p = 1:1:N-1     % all elements except the BHA
    if u(o,p)< 0    % check if the element is out of the annulus
       my_kinetic(o,p) = 0.2;
    else
       my_kinetic(o,p)=0.3-0.02*Circ+0.04.*R1(o,p)-0.02.*R2(o,p);
    end
  end
end

% COEFFICIENT OF FRICTION WITH NO EXPANSION INSTALLED:

for q = 1:1:M  % BHA has larger friction due to its larger diameter
  if u(q,N-1)< ext0(2) && u(q,N-1)> ext0(3)
     my_kinetic(q,N) = 0.87-0.05*Circ+0.04.*R1(q,N)-0.03.*R2(q,N);
  else
     my_kinetic(q,N) = 0.80-0.05*Circ+0.04.*R1(q,N)-0.03.*R2(q,N);
  end
end

%COEFFICIENT OF FRICTION WITH EXPANSION INSTALLED:

%for q = 1:1:M  % BHA has larger friction due to its larger diameter
%  if u(q,N-1)< ext1(2) && u(q,N-1)> ext1(3)
%    my_kinetic(q,N) = 0.8-0.05*Circ+0.04.*R1(q,N)-0.03.*R2(q,N);
%  else
%    my_kinetic(q,N) = 0.80-0.05*Circ+0.04.*R1(q,N)-0.03.*R2(q,N);
%  end
%end

for t = 2:1:M       % BHA
    if u(t,N) == u(t-1,N) && t < (M-5)
        c = c + 1;
        Fdrag(t,1)=Circ*(OD_BHA/(D(t,N)- OD_BHA))*pi()*Length_BHA...
            *visc_mud*(Velocity(t,1)-(pump_rate/A(t,N)));
        Ff(t,N) = my_static*mass_N*g*sin(Inclination);
    else
        Fdrag(t,1)=Circ*(OD_BHA/(D(t,N)-OD_BHA))*pi()*Length_BHA...
            *visc_mud*(Velocity(t,1)-(pump_rate/A(t,N)));
```

```
        Ff(t,N) = my_kinetic(t,N)*mass_N*g*sin(Inclination);
    end
end

for t = 2:1:M       % all elements except the BHA
    for n = 1:1:N-1
        if u(t,n) == u(t-1,n) && u(t,n) > 0
            c = c + 1;
            Ff(t,n) = my_static*mass_n*g*sin(Inclination);
        else
            Ff(t,n) = my_kinetic(t,n)*mass_n*g*sin(Inclination);
        end
    end
end

Fweight=mass_n*(N-1)*g*cos(Inclination)+mass_N*g*cos(Inclination);
div = 0;
tot = 0;

for i = 10:1:30
    if Velocity(i,1) > 0
        div = div+1;
        tot = tot + Velocity(i,1);
    end
end
average = tot/div;  % average drill string velocity
aks_motor = average/1.7;    % m/s2, based on observations
v20(1:M,1) = 0;     % block velocity
v20(2,1) = Velocity(2,1);

for t = 3:1:M-1
    if Velocity(t+1,1) == 0
        v20(t,1) = 0;
    else
        v20(t,1) = v20(t-1,1)+aks_motor;
        if v20(t,1) > average
            v20(t,1) = average;
        end
```

```
    end
end

Fspring(1:M,1) = 0;
dt = TIME(2)-TIME(1);
v_avg(1:M,1) = Velocity(1,1);
x(1:M,1) = 0.2;
strekk(1:M,1) = 0;

for t = 2:1:M
    v_avg(t,1)=(Velocity(t)+Velocity(t-1))/2; % drill string velocity

    if Acceleration(t,1) > 0.01 || Acceleration(t,1) < -0.02
        dx(t,1) = ((v20(t,1)+v20(t-1))/2*dt)-(v_avg(t,1)*dt);
    else
        dx(t,1) = v20(t,1)*dt - Velocity(t,1)*dt;
    end

    x(t,1) = x(t-1,1)+dx(t,1);
    if x(t,1) < 0.2
        x(t,1) = 0.2;
    end

    strekk(t,1) = x(t,1) - 0.2;

    if t > 3 && Acceleration(t,1) > 0.02
        Fspring(t,1) = 0.8*k*dx(t,1); % 0.8 is correction factor
    elseif dx(t,1) < 0
        Fspring(t,1) = 0;
    else
        Fspring(t,1) = k*dx(t,1);
    end
end

[val pos] = max(Fspring(37:40,1));

if val > 0
    Fspring(pos+36,1) = Fspring(pos+36,1) + 50;
```

```
end

if Circ == 1
    [maxV pos1] = max(Velocity(10:30,1));
    [minV pos2] = min(Velocity(10:30,1));
    posMax = pos1+9;
    posMin = pos2+9;

    for t = posMax:1:posMin
       if Fspring(t+1,1) > 100
           Fspring(t+1,1) = 50;
       end
    end
end

sum_Ff = sum(Ff,2);
for t = 1:1:M
    sum_HKL(t,1) =Fweight+Fspring(t,1)+sum_Ff(t,1)+Fdrag(t,1);
end

% DRILL STRING PUSHING PHENOMENON:

if posMax > 0 && posMin >0
    for t = posMax:1:posMin
       sum_HKL(t,1) = 90;
    end
end

if Circ == 1 && posMax > 0 posMin > 0
    sum_HKL(posMax:posMin,1) = 90;
end
```